DEVELOPMENT AND EVALUATION OF TRANSPARENT ALUMINUM OXIDE

Final Report

1 July 1966 - 30 June 1967

Prepared by

W.H. Rhodes
D.J. Sellers
A.H. Heuer
T. Vasilos

Prepared under U.S. Naval Weapons Laboratory
Contract N178-8986

June 30, 1967

AVSSD-0415-67-RR

AVCO CORPORATION
Space Systems Division
Lowell, Massachusetts

DEVELOPMENT AND EVALUATION OF TRANSPARENT ALUMINUM OXIDE

Final Report

1 July 1966 - 30 June 1967

Prepared by

W.H. Rhodes
D.J. Sellers
A.H. Heuer
T. Vasilos

Prepared under U.S. Naval Weapons Laboratory
Contract N178-8986

June 30, 1967

AVSSD-0415-67-RR

AVCO CORPORATION
Space Systems Division
Lowell, Massachusetts

FOREWORD

This report was prepared by the Space Systems Division of Avco Corporation under U.S. Navy Contract N178-8986, entitled "Transparent Armor Protective Material."

The work was administered under the direction of the U.S. Department of the Navy, Naval Weapons Laboratory, Dahlgren, Virginia, with Mr. Louis Flaer, Code TDMC, acting as Project Manager.

This report covers work conducted from 1 July 1966 to 30 June 1967.

The writers are pleased to acknowledge the contributions of the following individuals to this program: R. Gardner and J. Curtin for ceramographic preparation; P. Daniel and J. Centorino for materials preparation; R.M. Haag and P. Berneburg for X-ray studies; and R.M. Haag and A.S. Bufferd for useful discussions.

ABSTRACT

This study was aimed at the development of transparent alumina by employing hot working techniques on polycrystalline Al_2O_3 at temperatures above 1400°C.

Polycrystalline alumina possessing high total and in-line visible light transmission was fabricated by a hot forging technique which included suitable recrystallization and annealing periods. The percentage of the billet that was converted to high transparency was strongly influenced by the presence of a strain gradient in the billet, and this in turn was related to the aspect ratio of the billet, surface friction of the billet-punch interface, and the creep resistance of the punches.

The high total transmission was a result of nearly complete pore removal, and was equivalent to the best randomly oriented polycrystalline alumina. The high in-line transmission (up to 60%) was thought to be a result of a strong basal crystallographic texture induced during forging by the predominance of basal slip as a deformation mechanism. The deformation and recrystallization steps were thought to be effective in pore removal by a mechanism such as shearing of pores due to grain boundary sliding or the nucleation of a new population of grains at pores and their subsequent removal by vacancy diffusion. Initial experiments to define the critical strain for recrystallization indicate that this value lies between 4-10% "engineering" strain. The room and elevated temperature bend strength of transparent material was equivalent to dense but opaque alumina of equivalent grain size.

TABLE OF CONTENTS

LIST OF ILLUSTRATIONS

LIST OF ILLUSTRATIONS continued

LIST OF ILLUSTRATIONS continued

LIST OF TABLES

I. INTRODUCTION AND THEORY

The objective of this program was to produce transparent alumina by a technique which would lend itself to the production of sizeable sheets approximately $\frac{1}{2}$ inch thick. Earlier work[1] had demonstrated that alumina single crystals having a volume up to 7 cm^3 could be grown in the solid state. The apparent growth method was the strain-anneal technique (described in a subsequent paragraph) which has been used to grow sizeable single crystals of metals.[2] This was proof that primary recrystallization could be induced in alumina, and thus a new* method of microstructure control was open to the processing of alumina. Two new processing techniques were suggested from this finding for producing the required specimens of transparent alumina. They are

1. to produce transparent single crystals by the strain-anneal technique, and
2. to hot press polycrystalline alumina with a strong crystallographic texture (where a large percentage of the grains have an identical crystallographic relationship to a specimen surface) which was expected to enhance in-line light transmission due to the suppression of birefringent scattering. The production of transparent alumina by either of these methods required an understanding of deformation and primary recrystallization in alumina.

Primary recrystallization can be defined as the growth of strain-free nuclei into a deformed matrix, the reduction in strain energy providing the driving force.[5] Nucleation is important but particularly difficult to study in the case of alumina because deformation, recovery, grain growth, and recrystallization are all occurring simultaneously. In metals, this area is still unresolved,

*It is important to mention that primary recrystallization has been observed by Stokes and co-workers[3] after tensile deformation of MgO, and that Rice and Hunt[4] have been examining hot extrusion in polycrystalline MgO and Al_2O_3.

and research is active (see Reference 6 for a recent review). However, as in deformed metals, it may be assumed that in alumina after hot working, there will be numerous nucleation sites present, particularly at grain boundaries, pores, deformation bands, and free surfaces, and that nucleation will not be the rate limiting step in primary recrystallization. Further, the number of nuclei (strain free grains) increases with increasing strain, and this accounts for the relationship shown in Figure 1--increasing deformation leads to a progressively finer-grained structure after recrystallization.

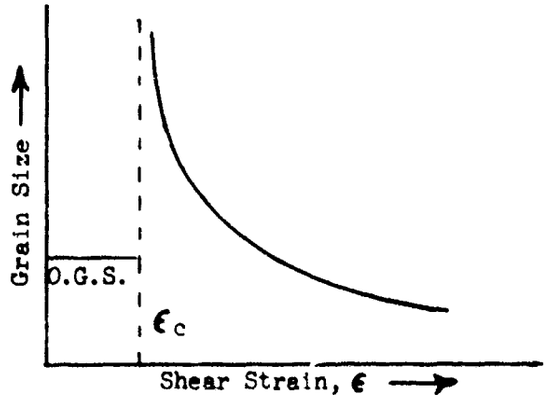

Figure 1. Variation of recrystallized grain size with deformation. Note that no recrystallization will occur below a critical strain, and sample will retain its original grain size (O.G.S.).

Microstructural evidence that this relationship holds was obtained in the examination of an alumina forging, Figure 2. This billet contains a radial strain gradient where the outer portions had been under the highest shear strain, and it is thought that the micrograph includes areas strained both below and above the critical strain, ϵ_c. The porous large-grained area to the left of the single crystal was near the center of the billet, and had not been strained sufficiently to undergo recrystallization. The single crystal almost certainly nucleated in a region of strain at/or just in excess of the critical amount, where the small strain prevented excessive nucleation. For

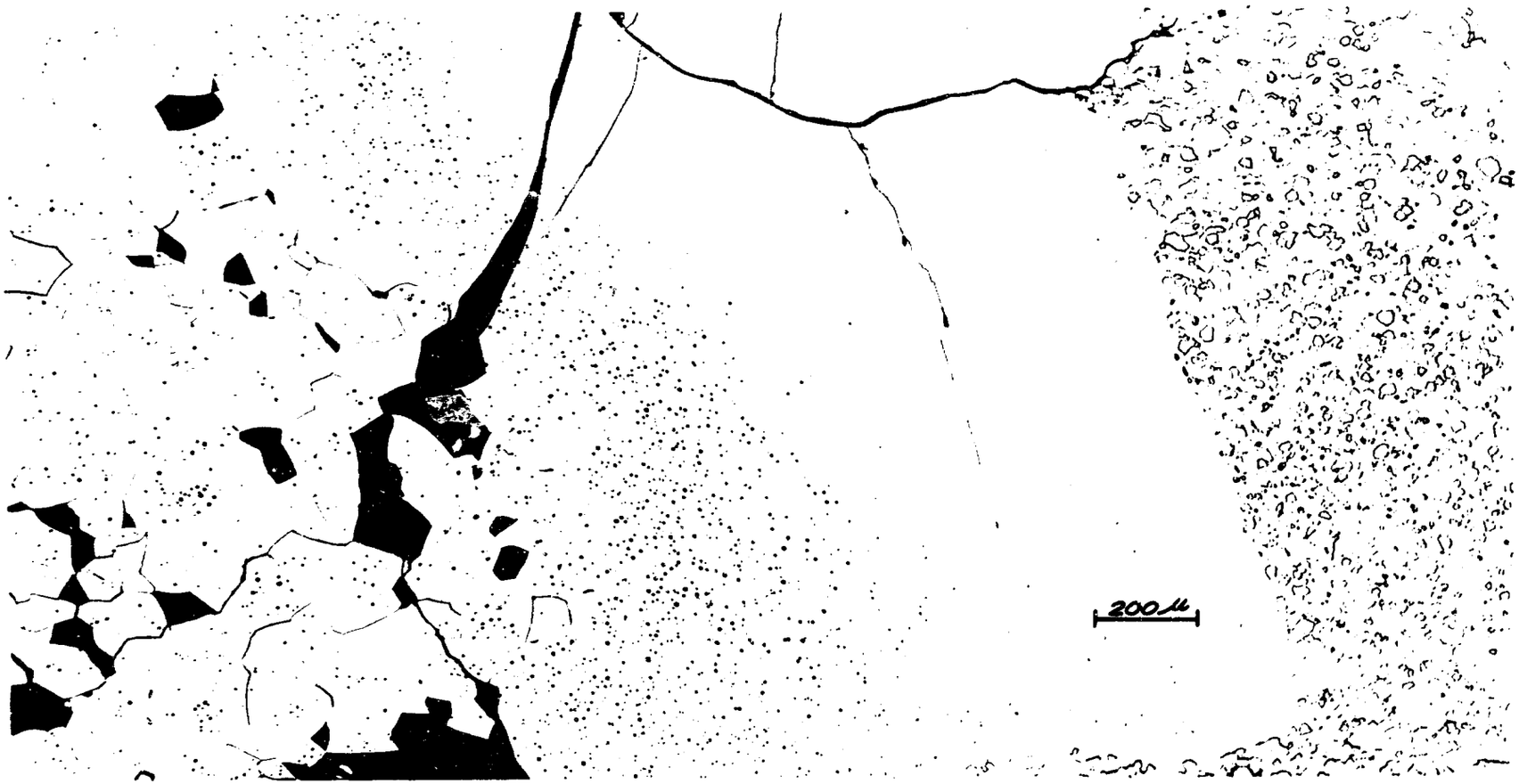

Figure 2.

Composite Micrograph Encompassing Coarse Unrecrystallized Area at the Left, a Single Crystal in the Center, and a Fine-Grained Pore-Free Structure at the Right

single crystal growth to be possible, growth of the first nucleus must proceed at such a rate that possible nucleation sites in adjacent areas are consumed. The area to the right of the single crystal had been deformed more extensively; hence, the nucleation rate was higher and recrystallization to a fine-grain matrix occurred before the deformed matrix was incorporated into the growing single crystal. When recrystallization to a fine-grained matrix was complete, the driving force promoting the fast growth of the single crystal was eliminated. The fine grain size of the right hand region is quite remarkable considering the long time this sample was subjected to high temperature and pressure (5 hours at 1870°C and 6000 psi).

The problem of single crystal growth by the strain-anneal technique (method 1 above) is somewhat more difficult than producing a recrystallized structure. The first aspect, of course, is to learn what amount of strain is in fact the "critical strain," ϵ_c, and then be able to induce just this amount of strain throughout a sizeable specimen. Deformation control is very difficult for alumina because all potential pressure transmitting die materials undergo creep and/or deformation at the temperature required (1750°C - 1950°C) for the deformation of alumina.* The second major problem is the control of the nucleation step. As mentioned in the previous paragraph, deformation is occurring above the recrystallization temperature. Therefore, after deformation, one must quench the sample to below the recrystallization temperature to prevent the nucleation of multi grains. Then, somehow the temperature of the sample must be raised in such a manner that one or perhaps several strain free grains nucleate. (One obvious technique is to pass the sample through a temperature gradient.) If several grains nucleate, preferred growth rates will usually allow one grain to

*One possible exception to this statement is the use of dense SiC die materials at 1350°C; this is discussed further in Section II.E.

dominate and consume most of the matrix.

It was recognized that the growth of large transparent single crystals by the strain-anneal technique would require a large amount of background research; even with this knowledge, process control and theoretical growth rates may preclude the achievement of sizeable crystals. Therefore, work on this process was aimed at answering one essential question about the strain-anneal process. What is the critical strain needed to induce primary recrystallization?

In principal, method 2 (above) which is illustrated by the area on the right of Figure 2 should be easier to produce than a large single crystal. Such a structure may well show improved in-line light transmission due to low porosity and perhaps crystallographic texture.

The previous study[1] demonstrated that highly worked alumina possessed a preferred basal crystallographic texture, so at the beginning of this project there was reason to believe that scattering of an image as it traversed through multi-grain boundaries could be greatly reduced for a worked body over a body of equal porosity but with random grain orientation.

To achieve a suitable recrystallized structure, an amount of shear strain should be induced uniformly in the specimen that is far greater than ϵ_c and preferably in the region where the recrystallized grain size-strain curve (Figure 1) becomes flat. Secondly, the specimen should be uniformly recrystallized; that is the temperature of the billet should be raised uniformly above the recrystallization temperature to allow simultaneous nucleation of the new population of grains. A uniform recrystallized grain size would have the best properties, and this would require a uniform strain; this property would be the most difficult to control in the hot working process. It was thought that the entrapped porosity problem would have to be approached separately; that is,

by first obtaining theoretically dense billet stock by either conventional pressure or pressureless sintering techniques. However, early in the program it was recognized from an examination of micrographs similar to Figure 2 that incorporated in the deformation-primary recrystallization process was a mechanism of porosity removal; note the decreasing porosity from left to right into the fine-grained recrystallized structure. Therefore, the elimination of these two light scattering mechanisms, porosity and anisotropic crystallographic texture were studied by considering a single process--hot working and recrystallization.

II. RESULTS AND DISCUSSION

A. Fabrication and Microstructural Characterization

The press forging and pressure anneal operations were conducted using the unconstricted die wall configuration shown in Figure 3. Three types of forgings were attempted; (1) forging of powder allowed to undergo normal sintering shrinkage during heat up to the forging temperature; (2) forging of precompressed, undersized cold pressed or partially hot pressed billets; and (3) forging of previously hot pressed or sintered dense material. The first two categories constitute a combination of hot pressing to full density followed by working of the ceramic material in its fully dense state. The third technique more closely represents a true forging wherein most of the vertical compression achieved results in plastic deformation of the material. Three types of Al_2O_3 powder having a purity of greater than 99.97% were employed; average particle sizes were 0.3, 0.05, and 0.06 microns.* The 0.3 micron powder was alpha phase Al_2O_3, while the 0.05 and 0.06 micron powders were gamma Al_2O_3.

The processing conditions for all the forging attempts conducted during the

*0.3 μ powder was Linde A, 0.05 μ powder was Linde B, and 0.06 μ powder was from A. Meller Co.

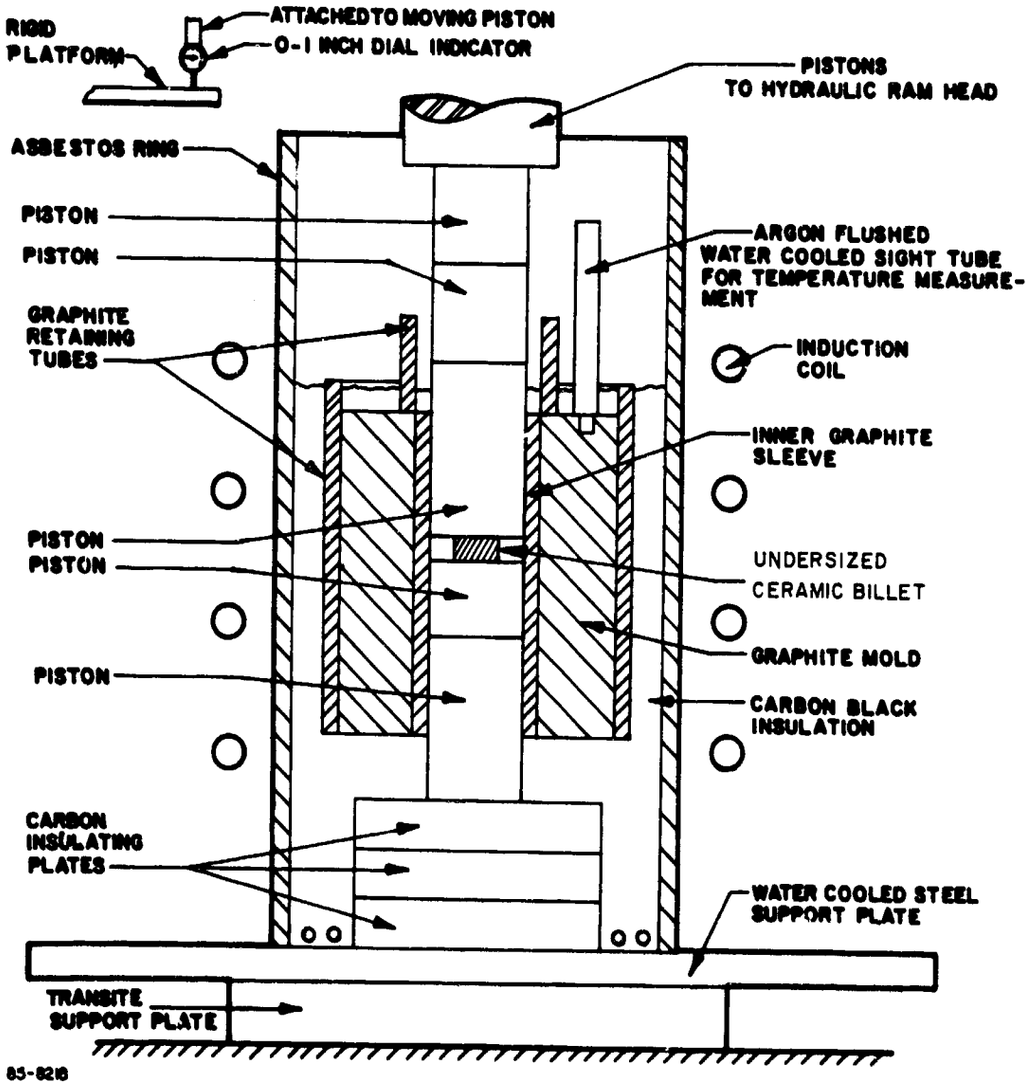

Figure 3 PRESSURE SINTERING APPARATUS USED FOR PRESS-FORGING EXPERIMENTS. NOTE THAT PRIOR TO FORGING, THERE IS NO CONTACT BETWEEN THE SPECIMEN AND THE DIE BODY

program are summarized in Table 1. As no quantitative data on the relative importance of the various process parameters was available at the onset of this study, a considerable effort was spent during the course of the experiments to single out several of the variables and to investigate their importance. The information gained from this approach as well as that from several alternative processing modifications incorporated into the program are summarized below. Appropriate definitions of optical terminology used in this report are found in the Appendix.

1. Powder Forgings

Figure 4 illustrates the progression of densification and deformation when powder was used as starting material for the forgings. The normal 3-inch diameter powder billet shrinks to approximately a 2-inch diameter during heat up and a density of 60% of theoretical is attained (top left piece in illustration; run FA-150). A similar run (FA-108) gave identical results. The application of 100 psi expands the diameter to $2\frac{1}{4}$ inches and the density to approximately 70% and 300 psi produces a piece of 2 3/8 inch in diameter and 80% dense (top middle and right billets in illustration; runs FA-151, 149). The application of further pressure produces further densification, lateral movement, and produces a piece with rounded edges similar in appearance to metal forgings (bottom left hand billet in Figure 4). Eventually the material fills the die and produces a dense straight edged piece with either conical surfaces or flat surfaces depending on the rate of deformation, the aspect ratio of the piece (height/diameter ratio), and surface friction. Further annealing under the proper temperature-pressure cycle produces recrystallization, and a change from opaqueness to transparency.

Table 1

Process Conditions for Forging of Transparent Al_2O_3

Billet No.	Powder Type	Forging Temp. °C	Forging Pressure (psi)	Time to Max. Pressure (min.)	Time at Max. Pressure (min.)	Height Differential from center to edge (%)	Relative Optical Density
FA-44	A(1)	1840-1860	4000	55	120	25	Transparent
FA-45	A	1810-1830	4000	45	215	< 5	Translucent
FA-46	A	1820-1860	5400	46	300	< 5	Translucent
FA-47	A	1850-1880	5400	35	335	< 5	Transparent
FA-96	A	1840-1870	5650	18	360	< 5	Top-Transparent Middle-White Bottom-Black
FA-97	A	1170-1840	5400	45	360	< 5	Slightly translucent
FA-98	A	1250-1840	5100	55	135	< 5	Slightly translucent
FA-100	B(2)	1860	5100	20	125	20	Translucent-Transparent
FA-101	B	1860-1870	5100-5400	25-35	320	30	Translucent-Transparent
FA-102	B	1340	5200	7-30	180	19	Top-Transparent Middle-White Bottom-Black
FA-103	B	1860	5400	15	180	-	Transparent
FA-104	B	1860	6000	20	180	< 5	Translucent-Transparent
FA-106	B	1870	6000	17	308	36	Outside-Transparent

Table 1 continued

Billet No.	Powder Type	Forging Temp. °C	Forging Pressure (psi)	Time to Max. Pressure (min.)	Time at Max. Pressure (min.)	Height Differential from center to edge (%)	Relative Optical Density
FA-107	B+C(3)	1870	6000	25	133	47	Outside-Transparent
FA-108	A	1860	-	-	5	-	Opaque
FA-109	A	1860-1880	6800	30	250	< 5	Transparent
FA-110	A	1860-1880	6800	20	230	< 5	Outside-Transparent
FA-118	A	1865-1880	6800	45-60	240	< 5	Translucent
FA-119	>99.5% (FA-118)	1860-1880	7000	35	215	No reduction	Translucent
FA-123	A	1310	2000		40		
FA-125	A-70% (FA-123)	1860-1880	25,000	30	180	< 10	Translucent-Transparent
FA-127	A	1850-1870	5100 5650 6200	15 8 (5)	83+30(N.L.)(4) 30(N.L.) 75(N.L.)	< 5	Outside areas-Transparent
FA-128	A	1840-1850	8700	15	240	< 5	Translucent-Transparent
FA-132	Lucalox	1850	15,000-17,000	30-45	180	5.4R(5)	Transparency improved by forging
FA-133	FA-119	1850	13,400	10-15	180	0-42.0R	Translucent
FA-135	>99.5% FA-12	1880-1890	20,000	5-10	125	73.5-80.6R	Transparent
FA-136	A+¼% MgO	1860	6000	22	143	< 5	Translucent, gray

Table 1 continued

Billet No.	Powder Type	Forging Temp. °C	Forging Pressure (psi)	Time to Max. Pressure (min.)	Time at Max. Pressure (min.)	Height Differential from center to edge (%)	Relative Optical Density
FA-137	A	1860	5650	15-17	380	< 5	Translucent
FA-140	A	1860	5400	24	71	15	Translucent
FA-141	A+¼% MgO	1860	5400	10-20	185	< 5	Translucent, gray
FA-142	A	1860	5670	20	30	26	Opaque
FA-143	>99.5% A+¼% MgO	1860	5650	10	230	< 5	Translucent, gray
FA-144	Lucalox	1860-1880	18,000	15	115	16-55R	Transparent
FA-145	Lucalox	1860	18,000	8	125	10-53R	Transparent
FA-146	Lucalox	1870-1880	18,000	321	180	35-50R	Transparent
FA-147	A	1860-1880	5650	48	360	< 5	Outside areas transparent-transl.
FA-148	A	1880	5650	30 + 77	318		Translucent
FA-149	A	1860	300	4	0		Opaque
FA-150	A	1860-1880	0	0	5		Opaque
FA-151	A	1865	100	2	0		Opaque

(1) A - Linde A - 0.3 μ particle size
(2) B - Linde B - 0.05 μ particle size
(3) C - A.Meller - 0.06 μ particle size
(4) N.L. - no load during annealing
(5) % reduction in height

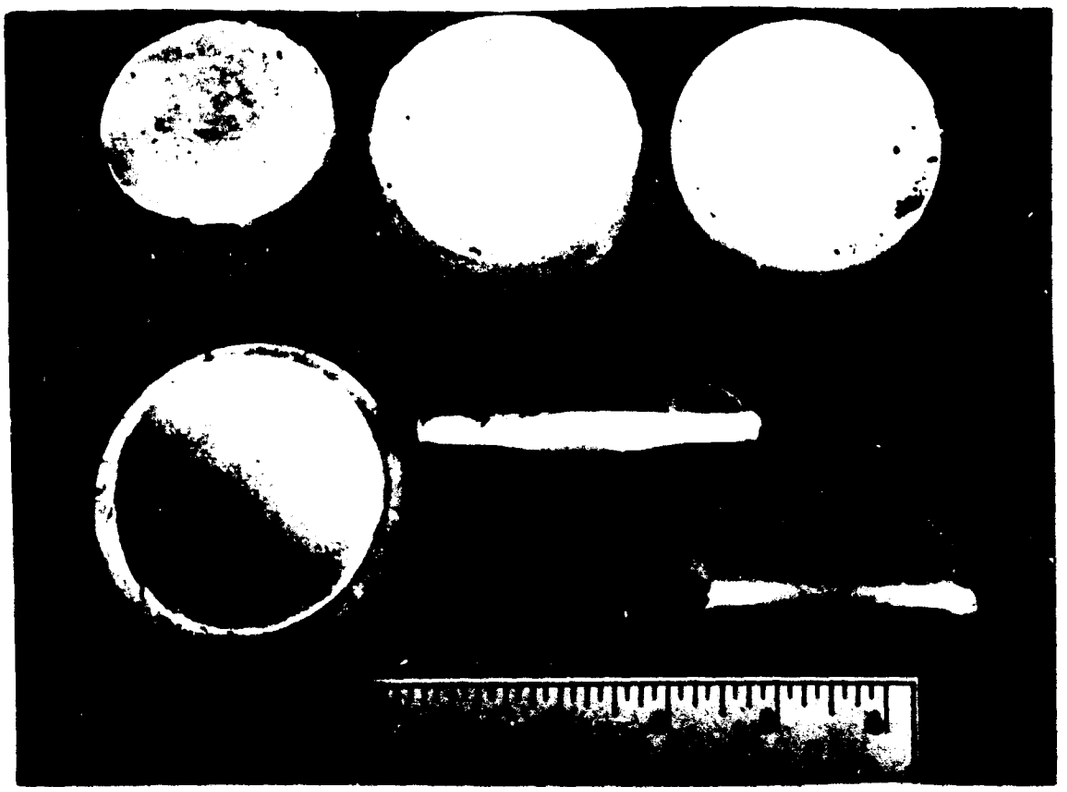

4500 2/3 X

Figure 4. Illustration of stepwise progression of material during powder forging.

a. Effect of Pre-Sinter, Forging Temperature and Length of Anneal

When employing raw powder billets, the usual procedure employed was to allow the billet to sinter and shrink under no load during heat-up and for a period of 2-5 minutes during which the temperature was stabilized prior to the application of pressure. One attempt (FA-148) was made to extend the sintering period for 30 minutes at zero pressure to see if such an approach was beneficial. The treatment appears to have promoted more extensive single crystal growth than normally experienced under these process conditions (Figure 5), and a large equiaxed microstructure containing entrapped porosity was produced in the polycrystalline section (Figure 6). It, therefore, appears detrimental to allow excessive sintering to take place before the advent of the deformation step. Similar conclusions were reached from run FA-97 and 98 which were pressure sintered rather than forged at temperature, pressure, and times normally employed to produce transparent material by forging. The forging condition (shrinkage to an undersized billet) was prevented during these runs by applying full load at lower temperatures. These translucent billets were found to contain very large, randomly oriented tabular grains with considerable porosity in the center of the grains and pore-free sections near the grain boundaries (Figure 7). The microstructure suggests that initial grain growth rates were large, and pores were entrapped. The time at temperature was sufficient, however, to allow the pores near the boundaries to be annihilated by vacancy diffusion to the boundary. The remaining porosity accounts for the lack of transparency in these pieces.

Forgings conducted between 1840° - 1900°C yielded the bulk of transparent material. One forging run (FA-45) conducted at 1810°C - 1830°C resulted in a translucent product and previous work involving long term forgings of Al_2O_3 below 1800°C were found to yield translucent products at best.

4500-A 1 X

Figure 5. Forging FA-148 showing two areas of extensive grain growth and translucent matrix.

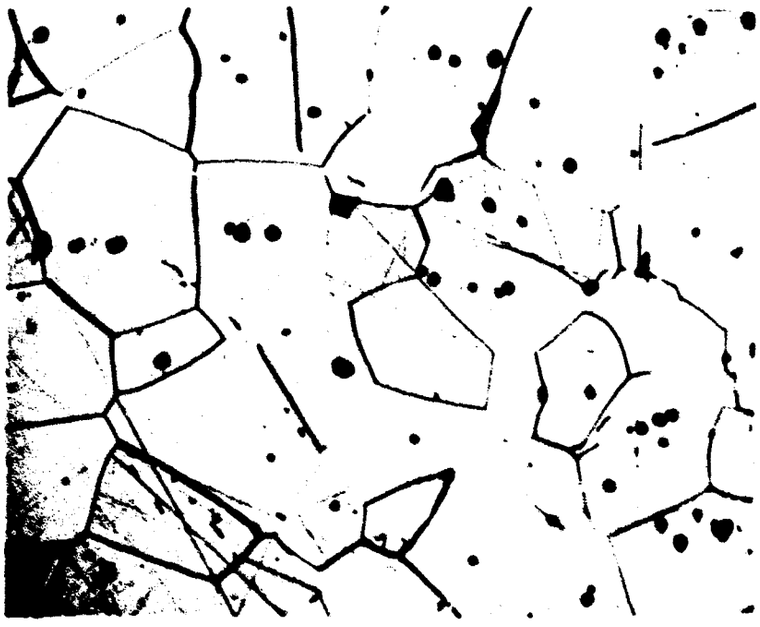

4503 250 X

Figure 6. Cross section of polycrystalline matrix of forging FA-148 showing retained porosity and equiaxed microstructure.

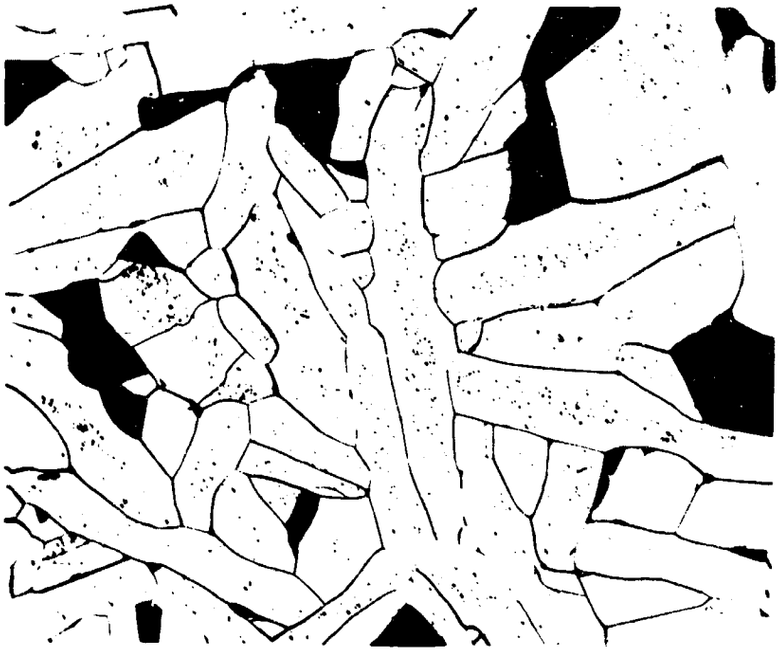

43570 100 X

Figure 7. Cross section of FA-97 hot pressed at 1840°C showing randomly oriented tabular grains with pore clusters laying in central areas.

Temperatures above 1900°C were found to result in the development of a single or small number of very large grains during recrystallization. The resultant anisotropy of thermal expansion between these grains and that of the surrounding finer grained matrix created sufficient internal stresses in the billets to cause crack propagation during the cooling cycle. Therefore, it seemed inadvisable to continue to hot form or anneal in the temperature range of 1900° - 1940°C. Process temperatures above 1940°C were not attempted as previous work has shown that the Al_2O_3 is likely to react severely with surrounding graphite media in this temperature range.

Temperature uniformity was found to be an important variable during the course of this program. This was discovered inadvertantly during run FA-96 when several graphite cylinders in the pressure train below the die body were replaced with one solid cylinder. This, of course, resulted in fewer interfaces in the vertical heat path and consequently a higher heat loss. The net effect was to produce a billet transparent on the top, white in the middle, and black on the bottom. As a check, the same effect was purposely reproduced in run FA-102 (Figure 8) by decentralizing the induction coil with respect to the die body causing uneven heating along the vertical axis of the die. The transparent section apparently experienced sufficient deformation to cause recrystallization which led to the transparent microstructure (Figure 9). The microstructural texture in the recrystallized matrix is thought to be due to preferential grain growth as it is well known that an anisotropy of grain growth rates occur in alumina. The recrystallized structure possesses the same crystallographic texture as produced during deformation[7] and it is well known that there is an anisotropy of grain growth rates in alumina. Figure 7 is an example of this where the grains were oriented randomly with respect to each other. The middle

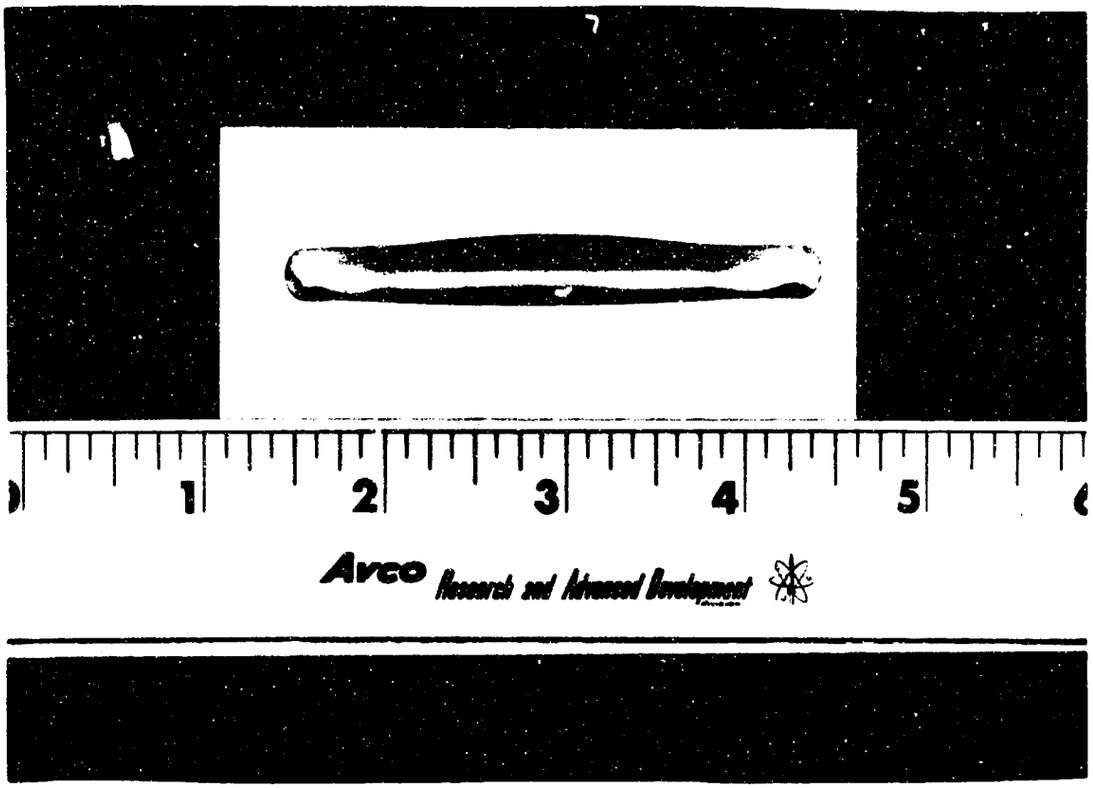

4500 A 1 X

Figure 8. Forging FA-102 forged under the influence of a steep temperature gradient

4502 D 750 X

Figure 9. Cross section of transparent area of forging FA-102

section of Figure 8 appears to have undergone recrystallization after less plastic deformation (due to the temperature gradient) as judged by the equiaxed and large grain size (Figure 10), but subsequent pore removal mechanisms were limited probably due to the temperature restriction. The cooler bottom section of the billet contained a much finer microstructure (Figure 11), and is thought to be the uncrystallized deformation microstructure. The black color apparently owes its origin to infiltration and condensation of carbonaceous gases.

Two short-term anneals conducted at 1860°C for periods of 30 and 70 minutes (runs FA-142, 140) failed to produce material of even good translucency. Runs FA-44, 100, 107 annealed for 120, 125, 133 minutes, respectively, established the minimum annealing period to produce transparency at 70-120 minutes. Runs FA-47, 96. 101, 106, and 147 with annealing periods of 308-360 minutes indicated that extended annealing up to 6 hours produces no detrimental effects on transparency. However, it is not yet clear if the long anneal is beneficial in improving porosity removal or crystallographic texture.

b. Effect of Starting Powder

The bulk of the experiments were conducted using Linde A, 0.3 μ alpha Al_2O_3, as the first encouraging experiments indicated that a pore-free material could be developed using this material. Six attempts (FA-100-106) were made later in the program to evaluate Linde B, 0.05 μ gamma Al_2O_3, and a sample amount of a third powder, A. Meller, 0.06 μ gamma Al_2O_3, was added to the top section of FA-107 to evaluate its potential. The 0.06 μ powder offered a distinct cost advantage over the 0.3 μ and the 0.05 μ powders. All three powders proved to be capable of producing transparent material under similar processing conditions. The A. Meller 0.06 , appears to have formed a more highly elongated grain structure than the Linde B powder in the same billet as shown in Figures 12 and 13, both taken near the surfaces of the

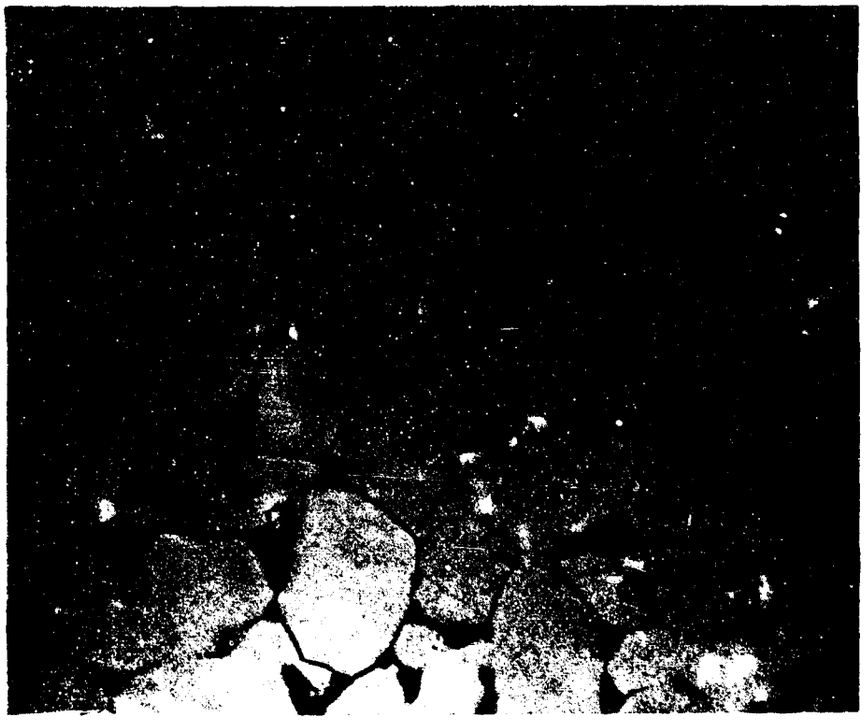

4502 C 750 X

Figure 10. Cross section of white area of forging FA-102 showing extensive porosity in grain boundaries.

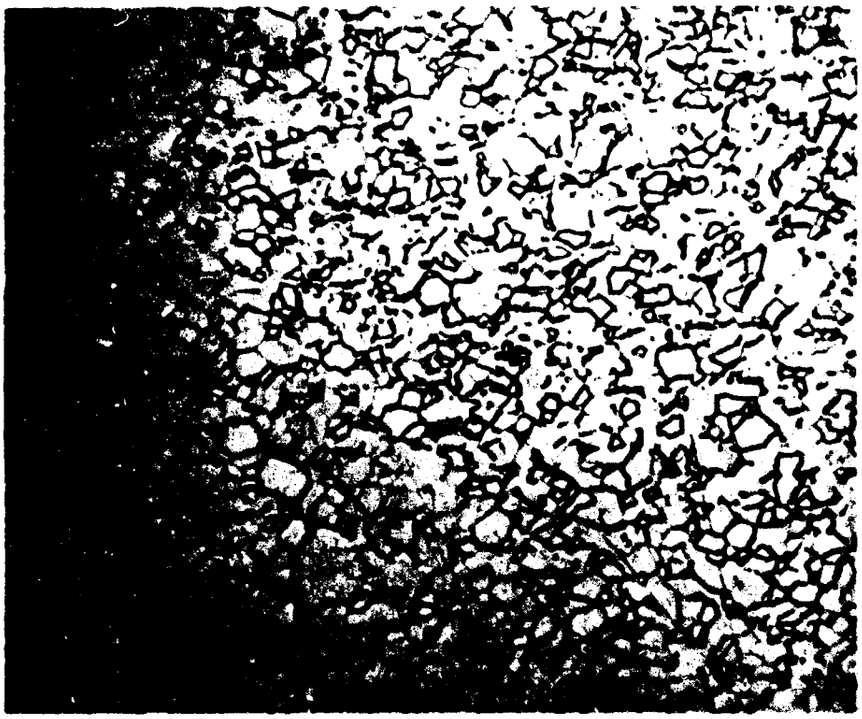

4502E 750 X

Figure 11. Cross section of dark area of forging FA-102 showing fine grained equiaxed grain structure

14503 B 250 X

Figure 12. Cross sectional area of forging FA-107 from area made from 0.06 micron gamma Al_2O_3 powder.

14503 C 250 X

Figure 13. Cross sectional area of forging FA-107 from opposite side of sample made from 0.05 micron gamma Al_2O_3 powder.

billet. Limited experience on conventional hot pressing of this material also indicates that it assumes a more tabular characteristic during grain growth, so it appears that this powder may offer some inherent characteristics that makes it more suitable for producing strongly oriented, low birefringent material. Further evaluation of this material during the report period was not possible, however, since a very small sample amount was available and the analysis of this sample was completed late in the program.

c. Secondary Effects on the Realization of Transparent Material

Several factors influenced the relative amount of polycrystalline material within the billets that attained a high degree of transparency. Many of the billets ended up with a domed appearance, and these billets experienced a gradient in strain history increasing from the center to the edge. The extent of doming in these specimens can be judged by referring to the differential (center to edge of the billet) in height reduction in Table 1. Transparency invariably was realized only in the outer sections of such billets. When the forgings resulted in a relatively flat specimen, the degree of transparency was found to be more extensive and uniform.

The areas of maximum strain (transparent areas in the domed specimens) contained a finely grained equiaxed or elongated microstructure as a result of recrystallization and in some cases the outer portions appear to have undergone exaggerated grain growth (Figure 14). Directly interior to this section was an area of very large grains or a single grain which was brought about by total strain slightly above the critical amount needed for primary recrystallization. The translucent center of the billets contained a microstructure of large equiaxed or tabular grains with abundant porosity and represent the product of insufficient total strain to cause recrystallization

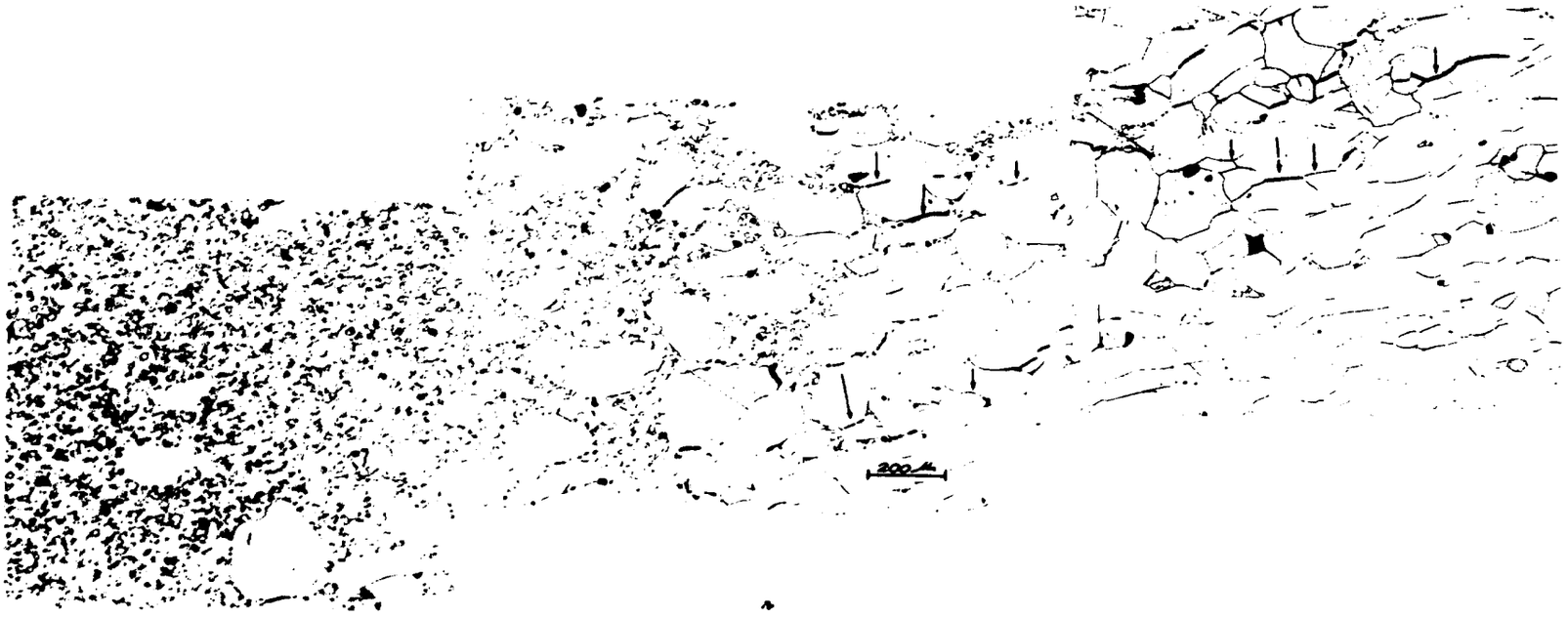

Figure 14. Composite photograph showing population of large grains toward the outside of forging FA-106. Note the radial gradient in the number and shape of large grains. The arrows point to porosity that may have been migrating along a strain or thermal gradient.

(also refer to Figures 1 and 2). The strain gradient found in these specimens is caused by a multitude of factors such as the hydrostatic stress distribution in the powder during uniaxial compression, surface friction on the punch faces encountered by material moving outward, the creep resistance of the mating punch material, and the strain rate employed. The effect of these factors on powder as well as solid billet forgings was investigated in a concurrent program[7]. Basically, hydrostatic pressure distribution was found to be influenced by the aspect ratio of the piece (height/diameter) and at very low aspect ratios (below 0.03), deformation becomes impossible. At slightly higher ratios, "doming" occurs, and intermediate aspect ratios yielded fairly flat forgings. Excessive height/diameter ratios would probably introduce new problems in the form of barreling of the piece and also by possible interior intergranular separations of material (due to excessive tensile forces). During many pressings, mutual gorging on the surfaces of both the molybdenum spacers and the Al_2O_3 occurred (for both solid and powder billets) and was undertaken as evidence for extreme surface friction. Attempts were made to evaluate pyrolytic graphite paper and a BN wash as lower-coefficient of friction surface materials for improved lateral extension of material (FA-45, 46, and 104). Both of these materials were effective as evidenced by the flat forgings produced. However, these separators should be looked upon with some reservation as the pyrolytic graphite caused limited reaction and inclusions in the surface, and the BN appears to have caused excessive grain growth along the surfaces of the Al_2O_3. A stronger grade of graphite (Poco ATX) was utilized in forgings FA-109, 110, 118, 125, 127, and 128, and was found effective in reducing the strain gradient over that normally realized with ATJ grade graphite at these temperatures.

Two forgings (FA-136 and 141) of the composition Al_2O_3 + ¼% MgO were attempted under conditions found to produce transparency in pure Al_2O_3.

It was of interest to see if this composition was capable of producing transparency with the possible added benefit of restricting recrystallization and/or grain growth to the point where the detrimental effects of large grains would be limited. (This additive has been found to be a very effective grain growth inhibitor and is responsible for the almost complete removal of porosity in the Lucalox sintering technique.) An examination of the microstructure of FA-136 (Figure 15) revealed that this composition successfully eliminated excessive grain growth (no large grained areas were found in either FA-136 or FA-141). Furthermore, attempted anneals at high temperatures (1900°C) on this piece produced only normal grain growth. The composition, however, resulted in a gray discoloration in the material and promoted enough reaction with the surrounding graphite during the long annealing periods to cause bonding and subsequent cracking during the cooling period.

2. Forging of Hot Pressed and Sintered Billet Stock

One possible disadvantage of the powder forging technique is that, due to the combined densification and deformation steps, there is limited opportunity to impart plastic deformation to the material; i.e., the powder column is very high due to the low bulk density of such fine powders and some lateral movement takes place before full density is achieved. A possible approach to overcome this limitation would be to use starting billets of moderate density (i.e., partially sintered or hot pressed) or to proceed directly to impart plastic deformation on undersized fully dense sintered or hot pressed material.

One attempt was made to test the feasibility of using 70% dense hot pressed material (FA-123) during run FA-125. The deformation of this material proceeded successfully, but no improvement was noted over that achieved

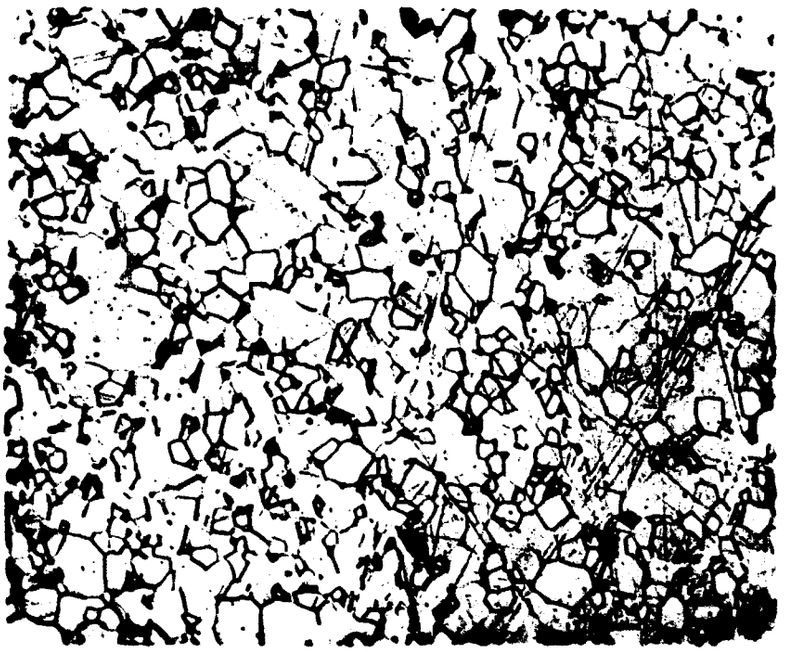

4384 250 X

Figure 15. Cross section of forging FA-136 of the composition Al_2O_3 + ¼% MgO.

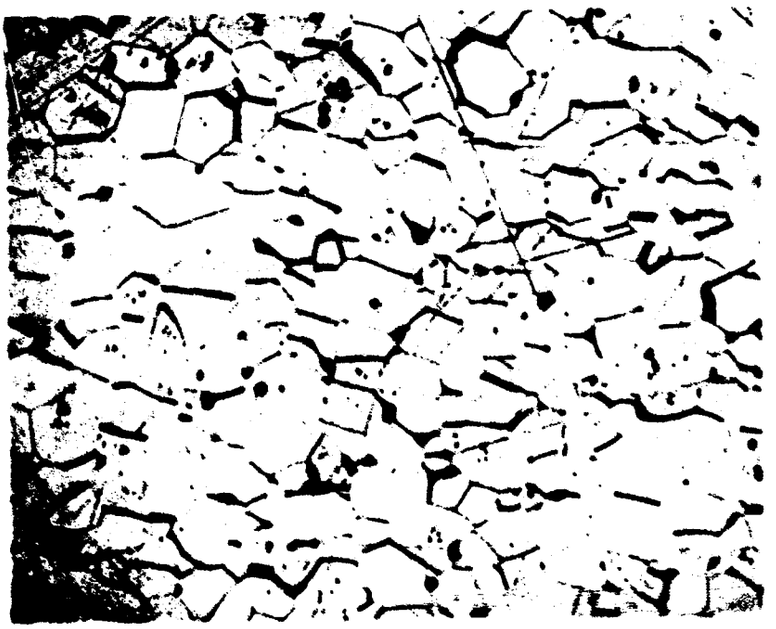

14503A 250 X

Figure 16. Cross section of forgings FA-125 made from 70% dense hot pressed billet. Note retained porosity

by powder techniques. Metallography revealed that an elongated grain structure was produced but entrapped porosity was noted in many of the grains. Apparently the pretreatment of this material (the initial hot pressing) creates further difficulties to the pore removal process that occurs during plastic deformation and annealing (Figure 16).

Several attempts at forging previously hot pressed or hot forged stock (FA-119, 133, and 135) revealed that slightly transparent material could be generated in this manner and that it took considerably higher pressures to produce a given deformation (little reduction occurred in FA-119 with pressures as high as 7000 psi). One attempt at a simultaneous multiple forging and annealing operation, FA-127, failed to show any improvement over the powder technique, and it is quite possible that only the initial pressure application produced plastic deformation with the material. An examination of the microstructure failed to show any evidence (texture) of extended plastic deformation. Another forging (FA-143) which was conducted on a dense, previously hot pressed billet of the Al_2O_3 + ¼% MgO composition (2.5 μ grain size) experienced a 46% height reduction at pressures close to those normally employed in the powder forging. The ease of forging a dense billet was strongly dependent on grain size (the smallest grain size forges the easiest - lowest pressure).

Several attempts (FA-132, 144, 145, and 146) were made at forging Lucalox material. This material is nearly pore free, thus forging is only needed to impart crystallographic texture to improve the transparency. Here again, it was found that very high pressures were needed to cause deformation presumably because of the large grain size. Some improvements in optical properties were realized in FA-132 over unforged material (see Section II.D), but an examination of billets FA-144, 145, and 146 revealed that elongated grain structures were not attained in any portion of the billets (Figures 17).

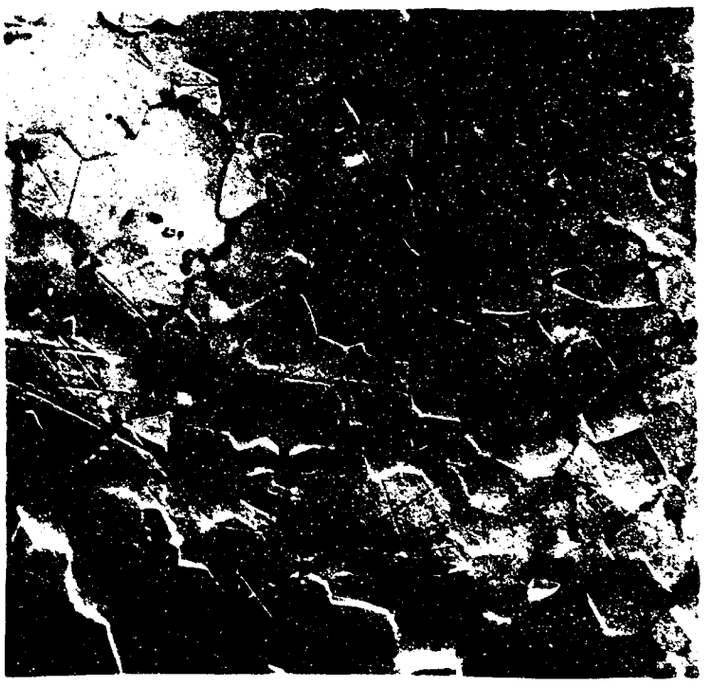

14448D 250X

Figure 17 Section of forging FA-146 (Lucalox), perpendicular to the plane of pressing. Note spinel phase.

These specimens have not been fully characterized for crystallographic texture. Perhaps the only improvements in optical characteristics are due to further pore removal by the simultaneous application of pressure and temperature (see Section II.C). A comparison of the differential in height reduction of FA-144, 145, and 146 (Table 1) versus time to maximum pressure shows that some reduction in the "doming" of these pieces can be brought about by a reduction in the strain rate.

The difficulty of forging dense billet stock is apparently due to the large initial grain size. This conclusion is strengthened by the realization that high pressures, $>$ 10,000 psi, were never found to be necessary when forging dense, 5 μ grain size pieces of hot pressed Al_2O_3 + $\frac{1}{4}$% MgO.[7]

B. X-Ray Diffraction Studies

Diffraction scans were conducted on sections of transparent billets, both parallel and perpendicular to the pressing direction, and the results were normalized to characterize the degree of preferred orientations produced during the forgings. This was done by comparing the peak intensity levels received from the crystallographic planes in forged specimens to the published values expected from randomly oriented powder samples. This measurement is thought to be important in the evaluation of transparent material as a high degree of crystallographic texture is expected to reduce scattering due to birefringence.

The hot forging work was found to generate material in which appreciable amounts of preferred crystallographic orientation was observed. This is shown in Table 2 which lists the normalized intensities for the basal planes (0006) and (000.12) a plane close to the basal plane with favorable Bragg conditions for strong reflection ($10\bar{1}.10$) and the prism planes ($11\bar{2}0$) and ($03\bar{3}0$)

Table 2.

Relative Intensities of X-Ray Reflections From Indicated Planes in Forged Al_2O_3

		Basal Planes			Prism Planes	
Sample No.	Direction	(0006)	$(10\bar{1}.10)$	(000.12)	$(11\bar{2}0)$	$(03\bar{3}0)$
Randomly Oriented Powder		1	15	3	40	50
FA-45	Parallel	0	66	17	15	19
	Perpendicular	0	5	28	77	100
FA-47	Parallel	8	100	18	12	1
	Perpendicular	0	6	0	100	73
FA-103	Parallel	0	11	0	0	0
	Perpendicular	2	8	2	79	58
FA-106	Parallel	36	63	15	47	16
	Lg. Grain Perpend.	0	0	0	100	27
	Sm. Grain Perpend.	2	6	0	47	81
FA-107	Parallel	14	77	14	12	18
	Perpendicular	5	0	0	79	67
FA-109	Parallel	5	9	2	6	8
	Perpendicular	0	6	0	70	90
FA-110	Parallel	5	24	9	4	3
	Perpendicular	0	8	0	40	71

for Al_2O_3. If orientation was not achieved during the working and annealing periods, the intensities in both sections would be similar and match that of the randomly oriented powder pattern listed at the top. As can be perceived from the data, intensity values are enhanced for the basal planes in sections parallel to the pressing direction and for the prism planes perpendicular to the pressing direction. The overall effect is that the process yields a product in which an abundance of grains are oriented with the c-axis running through the thickness of the piece.

It is thought that the crystallographic texture arises principally from the dominance of basal slip, $(0001)\langle 11\bar{2}0\rangle$ during the plastic deformation. This texture arises as the basal planes rotate, due to a superimposed bending moment, into a stable position normal to the compressive force. Other modes of deformation must occur to satisfy the Von Mises criteria of five independent slip systems; otherwise, voids or cracks would be generated. Twinning, grain boundary sliding, diffusional creep, and slip by other slip systems are all possible. Prismatic plane slip, $(11\bar{2}0)\langle 10\bar{1}0\rangle$, has been reported to occur above 1600°C, and previous work[1,7] has indicated that rhombohedral slip $(\bar{1}0\bar{1}2)\langle 10\bar{1}1\rangle$, probably also occurs during the forging of alumina. This latter slip system is as yet not well documented.

The crystallography of the deformed structure is unchanged upon recrystallization, and this may be due to oriented nucleation or oriented growth of the recrystallized grains. Figures 18 and 19 show the microstructures of two specimens exhibiting a high degree of transparency (see Section II.D for optical properties). Both specimens are large grained, 40 μ to 100 μ, and both show crystallographic texture. However, billet FA-47 exhibited microstructural texture as well as evidenced by the elongated grain structure (Figure 19). The most consistent explanation of the recrystallization process that evolved from

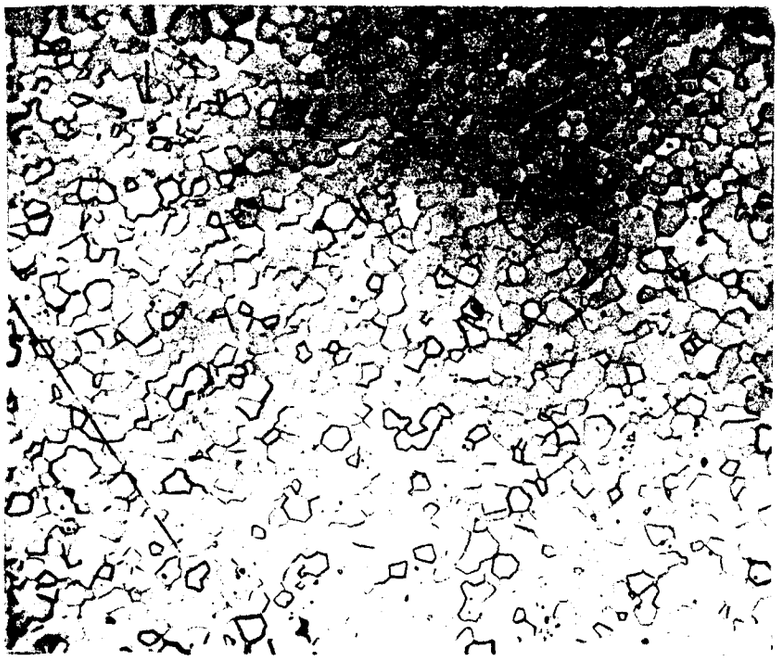

4358D 100 X

Figure 18. Cross Section of transparent section of forging FA-110 perpendicular to plane of pressing.

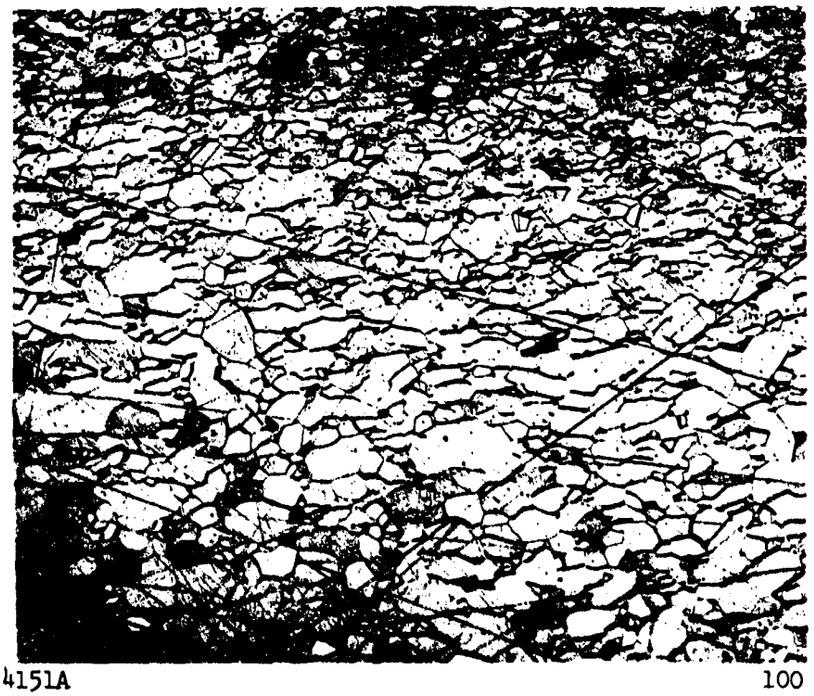

4151A 100 X

Figure 19. Cross Section of transparent section of forging FA-47 perpendicular to the plane of pressing.

related work[1,7], and can also be deduced from examing these structures is the following:

Both structures are recrystallized. The new generation of grains retains the crystallographic orientation of the deformation structure due to oriented nucleation. FA-110 received a light deformation and it recrystallized to a coarser structure than the more heavily deformed FA-47 (following the relation shown in Figure 1). FA-47 attained a microstructural texture by preferential grain growth (it already had a crystallographic texture due to recrystallization). This type of structure only occurs if the structure recrystallized to a very fine structure and/or the grains have grown very large.

C. Pore Removal

The driving force for the removal of porosity by solid state diffusion is the decrease in surface free energy by the elimination of the solid-vapor interfaces. Atomistically, the process is best viewed as the movement of ions to the pore and the counter migration of vacancies to either a free surface or a grain boundary sink (the latter is by far the most important of other possible sinks). This process is believed to be the major mechanism leading to densification in either pressure or pressureless sintering of Al_2O_3[9,10]. Pressure sintering occurs at lower temperatures than ordinary sintering because the pressure increases the vacancy gradient (causes more rapid diffusion) between the pore and sink. As was mentioned in Section I, there is an apparent pore removal mechanism operating in conjunction with primary recrystallization. Possible explanations for the observed phenomena will be discussed in light of known sintering and recrystallization phenomena.

The porous microstructure to the left of the single crystal in Figure 2 is an example where the grain growth rates and consequently grain boundary

velocities were high enough to isolate pores sufficiently far from grain boundaries so that they could not be removed by subsequent diffusion of vacancies during the annealing period. It appears that in the recrystallized (right) area in Figure 2 (forged from powder), either the deformation or the subsequent recrystallization must have been effective in removing pores. The entrapped porosity in the left of the single crystal of this figure suggested that the movement of a grain boundary during recrystallization may itself not be a particularly effective way of removing porosity, even if that grain boundary intersects a pore. This is not surprising, as a similar situation arises in pressureless sintering, whenever exaggerated grain growth occurs; porosity becomes entrapped because the mobilities of the grain boundaries of growing secondary grains are high enough to allow them to sweep past pores.

One possible explanation is that the deformation during hot working contributes to removal of porosity. The observation that the decreasing porosity gradient in Figure 2 seems to parallel the increasing strain gradient is evidence for this. The exact mechanism of porosity removal during deformation is not known with any certainty, but the following may be suggested:

1. Pre-Recrystallization Mechanisms

   a. Rapid diffusion of ions and counter diffusion of vacancies from isolated pores to grain boundaries could occur by "pipe" diffusion along the many dislocations present after working.

   b. The deformation of the matrix could destroy the size and shape of pores, thereby altering and very possibly increasing the driving force for pore removal.

   c. Grain boundary shearing and sliding could destroy the geometry of pores lying along the boundary. Theoretically, the pore could be spread out as a flat platelet until they essentially become

adsorbed "into" the boundary.

d. Pores may be able to close by self welding under an applied load if the entrapped gas has a sufficient solubility in the matrix.

2. Recrystallization Mechanisms

a. The new population of grains may recrystallize at pores, thus making the diffusion distances short for vacancy diffusion.

b. The recrystallized grains are, of course, angstrom size at some point, and they may well be nucleated randomly in the structure. As the grains grow they will come in contact with the remaining pores. The boundaries may become pinned by the pores as they grow and/or the pores could be adsorbed by the grain boundary during growth.

It would appear that further theoretical work is needed to ascertain if any of these mechanisms (or others) may be important in the present process. However, while rapidly moving boundaries of recrystallizing grains may not be able to remove porosity, the recrystallized structure may be much more suitable for subsequent densification than the original matrix (mechanism B-2). Such a situation is suggested by some of the work with powder billets. Quenching a forged powder billet as soon as the rate of punch travel has slowed down ($\sim \frac{1}{2}$ hour) led to a porous, partially recrystallized microstructure; this is shown in Figure 20. However, leaving such a billet under temperature and pressure for long times (2-6 hours) leads to the dense optically-transparent polycrystalline specimens shown in Figure 21. The transparency is, of course, excellent evidence that all porosity was removed, as any remaining pores would scatter light.

Figure 20. Porous recrystallized microstructure "quenched" after forging for $\frac{1}{2}$ hour.

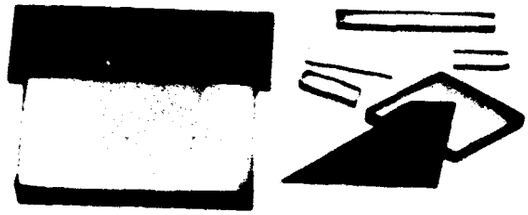

16386-C

Figure 21. Transparent alumina produced by hot forging.

D. Optical Properties

Sapphire is trigonal and consequently all of its physical properties are expected to be anisotropic and vary with the direction of measurement relative to the major crystal axes; in particular, differences are prevalent between the C and the A axes. The optical properties of sapphire show this anisotropy and consequently are subject to certain restrictions. Light entering a single crystal at some arbitrary direction to the main crystallographic axes is split into two rays, traveling with different velocities and vibrating in different directions. One of the rays vibrates in a plane defined by the direction of travel and the C axis, while the other vibrates in a direction normal to this plane. The two rays are known, respectively, as the extraordinary and ordinary ray. In sapphire, the ordinary ray has a slower velocity; sapphire thus falls in the optical category of uniaxial negative and two indices of refraction exist for the two rays. The only exception to this splitting of light into two components is for light incident on the basal plane. In this case, all rays are vibrating in a direction normal to the C axis.

Polycrystalline alumina would be subject to the optical property restrictions of the parent crystal. If the crystallites were randomly oriented, a beam of white light would be split many times passing through the thickness of a specimen. However, if the C axis of the crystallites in a polycrystalline body were perfectly aligned (the A axes could have a random relationship to each other), light would not be split when viewing parallel to the C axis, and would only be split once into the ordinary and extraordinary rays when viewed normal to this direction.

The losses in optical transmission are normally the accumulation of three effects; reflectance, scattering, and absorption. The reflectance loss, r,

(Frensnel losses) at an interface for sapphire with N = 1.76 is given by:

$$r = \frac{(N - 1)^2}{(N + 1)^2} = 0.077 \qquad (1)$$

where N is the refractive index. Therefore, the transmission at each surface is 0.923 and the transmission, T, for a sample with no other losses (theoretically impossible, of course) is given by:

$$T = (1 - r)^2 = (0.923)^2 = 0.852 \qquad (2)$$

When absorption losses are considered, the transmission is given by:

$$T = \frac{I}{I_o} \quad 100 = 100\ (1 - r)^2\ e^{-\alpha x} \qquad (3)$$

where

I = intensity of transmitted light

I_o = intensity of incident light

α = coefficient of absorption (cm^{-1})

x = thickness of sample in cm.

The absorption coefficient, α, varies with wavelength, and is thought to be "low" in the visual range, but it attains values as large as 1.9 to 7.6 cm^{-1} in the infrared range. In the visual range, samples of sapphire 0.0482 cm and 0.2573 cm thick possessed an equal transmission of 85%, and it could be inferred that thicker samples may equal this transmission level.

It was difficult to assess the differences between a translucent and a transparent specimen when they are both unpolished. However, an effort was made to select the "best" specimens from the large number fabricated, and a number of these were polished and their optical properties were determined in the visual range. Other specimens produced in the program will undoubtedly show equal and perhaps superior properties, and these will be subsequently examined.

The crystallographic texturing and possible consequences of texture on optical transmission have been discussed, so it is important to reference the samples predominant optic (C) axis; the sampling method is shown schematically in Figure 22. Each graph showing optical data refers to the x and y direction.

Figure 22. Orientation of Specimen for Optical Measurements

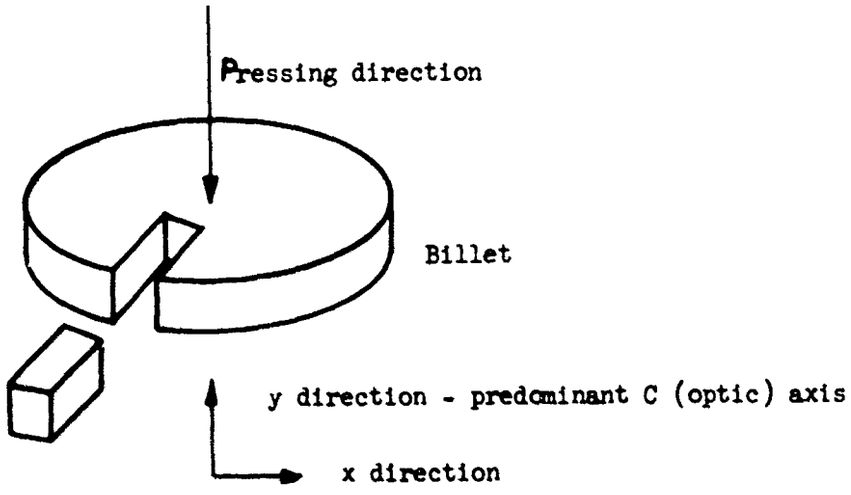

Both in-line and total transmission measurements were conducted with an extended range Beckman DK-2 ratio recording spectrophotometer. The instrument was calibrated before each series of tests using a National Bureau of Standards "Didymium" glass standard.

A number of both x and y samples were sectioned from billet FA-47 (forged from powder at 1860°C, 5400 psi, and 335 minutes). The total and in-line transmission (5° exit cone) is plotted as a function of wavelength in the optical range for x specimens of three different thicknesses in Figure 23. The total transmission for the 0.5 mm thick specimen approaches that found for sapphire of this thickness (85%). The in-line transmission of these samples exceeded any previous values reported for polycrystalline Al_2O_3 of comparable

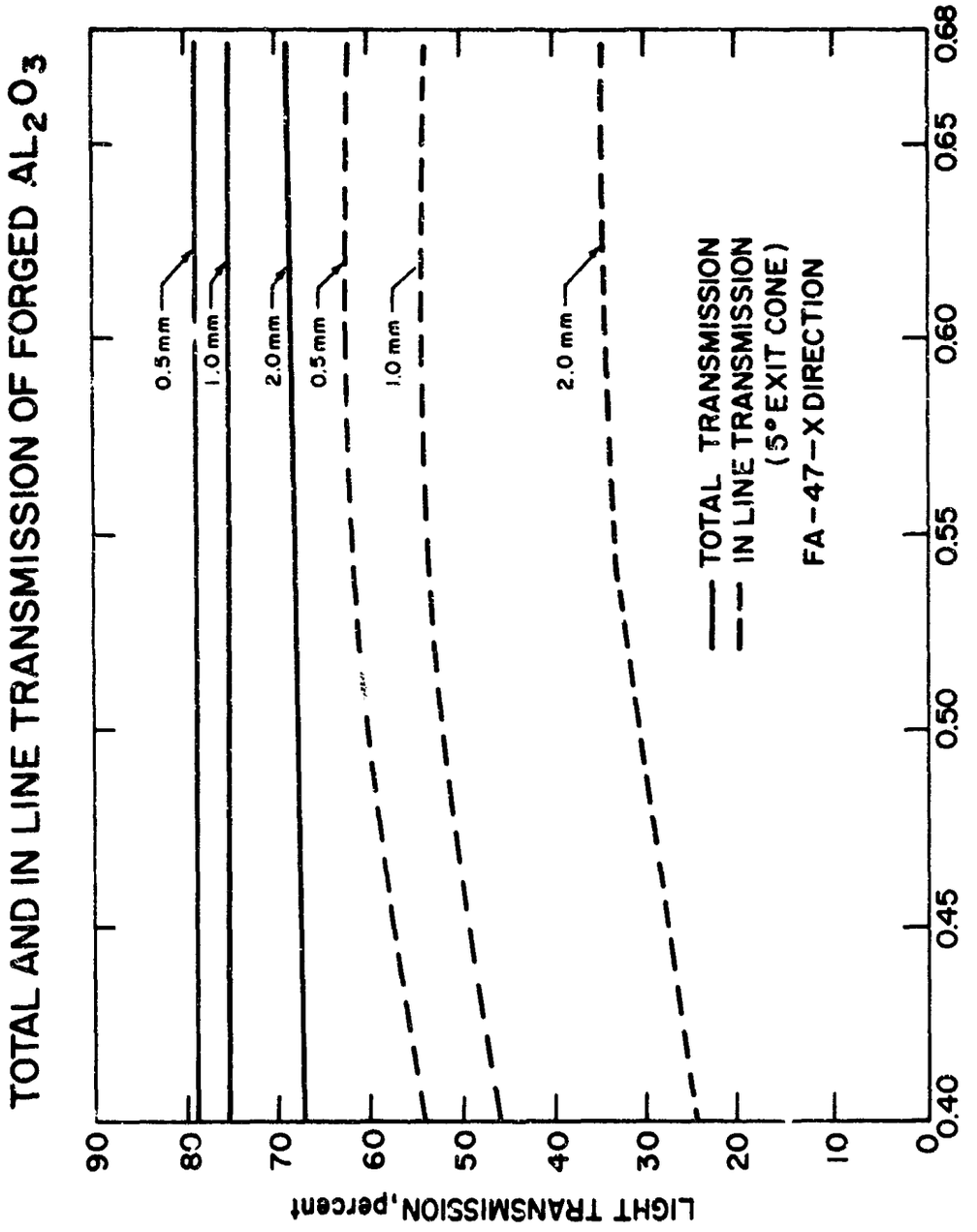

Figure 23 TOTAL AND IN-LINE TRANSMISSION FOR FORGED BILLET FA-47 TAKEN PERPENDICULAR TO THE PRESSING DIRECTION

thicknesses. R.L. Coble, holder of the initial Lucalox patent, reported values of 0.5% to 4.5% for 1 mm thickness in patent No. 3,026,210, and St. Pierre lists 40% maximum for 0.5 mm thickness in patent No. 3,026,117 for Lucalox material of improved in-line transmission.

Professor R.L. Coble kindly loaned his most transparent Lucalox sample to Avco for a direct comparison of the two materials. The total and in-line transmission values for this piece (Al_2O_3 + MgO) and for sections of forged material (FA-47) with faces parallel to the pressing direction (y) are shown in Figure 24. Sections of the forged billet taken in the y direction were found to contain slightly higher total transmission and considerably higher in-line transmission than those measured in the x direction.

For example, compare the Lucalox (Al_2O_3 + MgO) specimen with the slightly thicker (2 mm) forged specimen. The Lucalox piece has a very good total transmission (approximately 80%) while the forged material was slightly lower (approximately 70-72%). The in-line transmission of the forged material, on the other hand, was considerably higher (49% vs. 16%) than in Lucalox. The 1.8 mm thick Lucalox specimen possessed an in-line transmission about equal to that for the 4.8 mm forged Al_2O_3.

The in-line transmission differences are shown more dramatically in Figures 25 a and b. In Figure 25 a, the 1 mm forged, the 1.8 mm Lucalox, and the 2.0 mm forged pieces were placed against printed matter. All three pieces show good total transmission as evidenced by the intensity of the image received. In Figure 25b, the pieces were placed on a thin glass slide and raised approximately one inch from the printed matter. As can be seen, the image when viewed through the Lucalox becomes extinct due to birefringence while the image is still reasonably distinct through the 2 mm forged piece and essentially unaltered through the 1 mm forged piece.

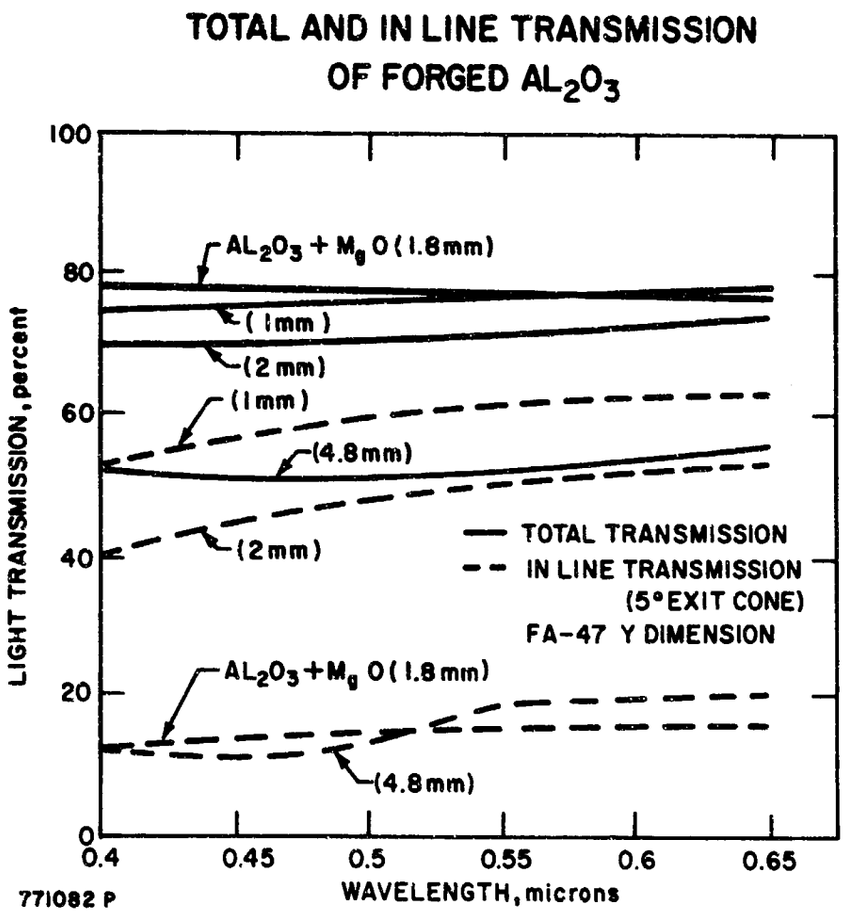

Figure 24 TOTAL AND IN-LINE TRANSMISSION FOR FORGED BILLET FA-47 TAKEN PARALLEL TO THE PRESSING DIRECTION

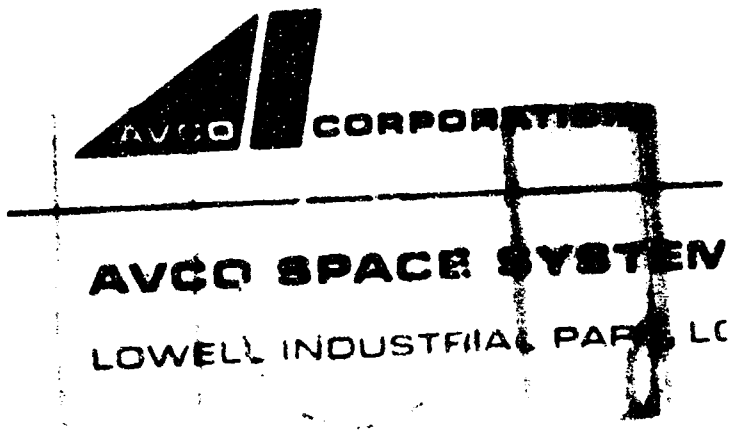

a

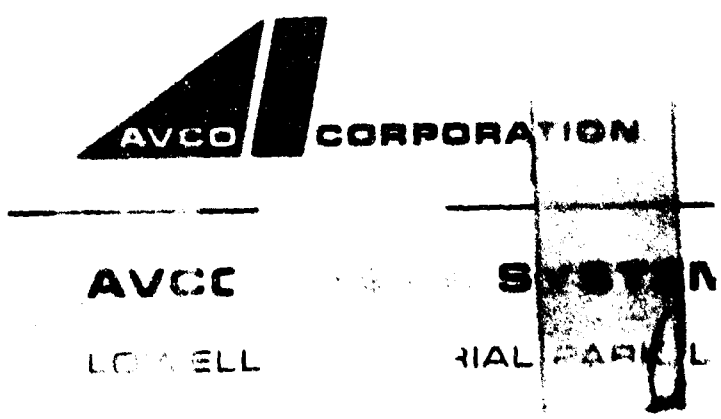

b

Figure 25. Comparison between optical transmission in forged alumina (left and right) and Lucalox (center). The samples are lying flat on the paper in (a) but raised 1" in (b).

The explanation for these results almost certainly lies in the crystallographic texture. Scattering at pores cannot explain these results, as the Lucalox specimens exhibited higher total transmission; thus, if scattering was dominant, the Lucalox in-line transmission should be higher than the forged specimen. Birefringence or the splitting of the ordinary and extraordinary rays as light passes through the multiple randomly oriented grains must account for the loss of in-line transmission in Lucalox as compared with the forged crystallographically textured samples. The texture of FA-47 was not perfect, of course, or otherwise the in-line transmission would have approached the total transmission. Also, it was noted that y samples exhibited slightly ($\sim$ 8%) greater in-line transmissions than x sample of the same thickness. Although there is a possibility that these were essentially "better" samples, the most reasonable explanation is that light passing through the x samples is split into the two rays and this results in further losses due to the interaction of these two vibrating modes with grain boundaries and any remaining porosity. Light passing through a y sample with perfect basal plane texture would not be split.

Total transmission curves for x specimens from billets FA-44 (forged from powder at 1850°C, 4000 psi, 120 minutes) and FA-110 (forged from powder at 1870°C, 6800 psi, 230 minutes) are presented in Figure 26. Billet FA-110 was the most transparent of the two, but both billets exhibited slightly lower values than FA-47 (see Figure 23 and compare the 1.0 mm and 2.0 mm curves). The x-ray data in Table 2 showed that FA-47 possessed a higher degree of basal texture than FA-110 which is undoubtedly part of the explanation. Some difference in porosity level may also be present although this could not be detected by immersion density measurements.

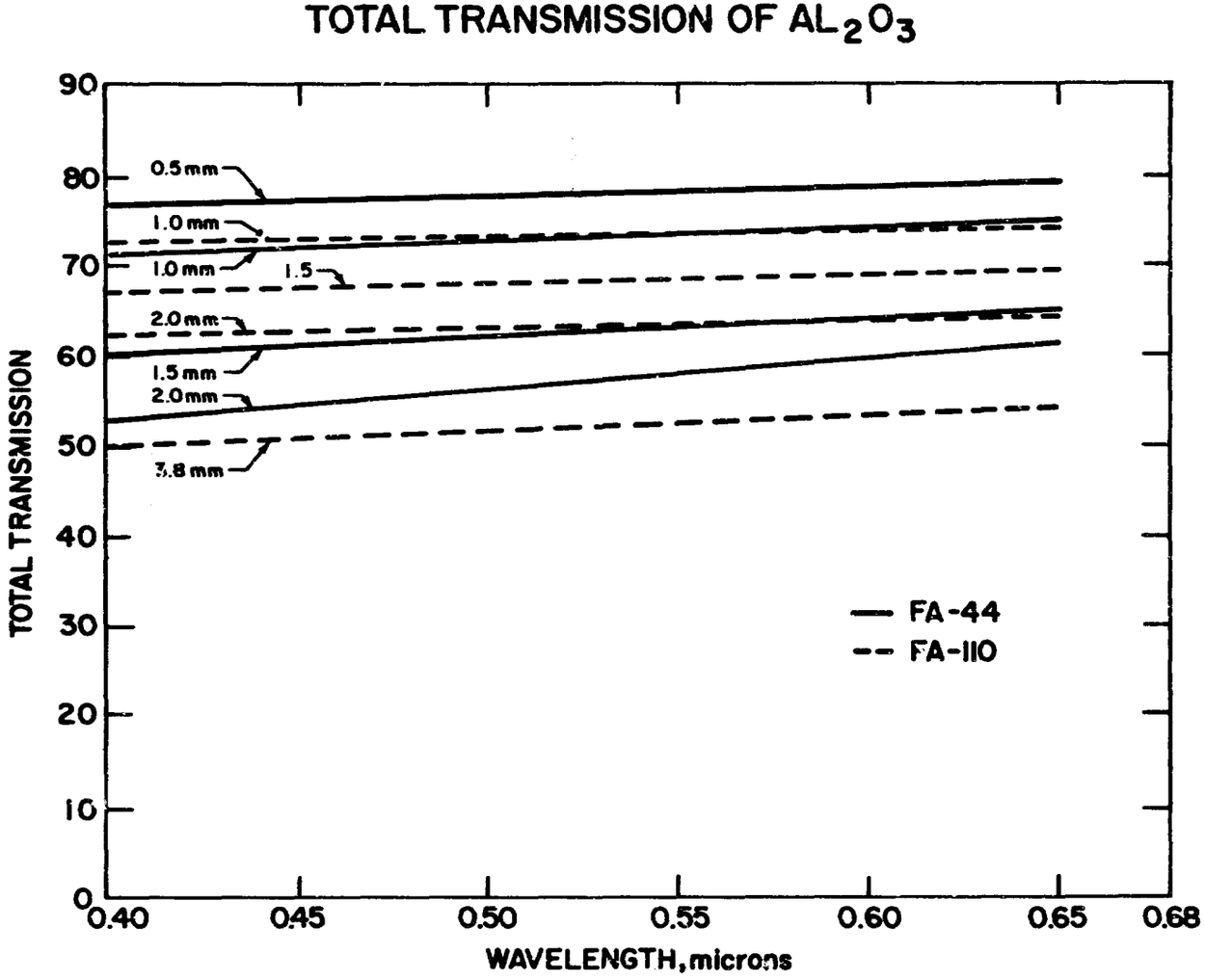

771084 P

Figure 26 TOTAL TRANSMISSION FOR FORGED BILLET FA-44 AND FA-110, TAKEN PERPENDICULAR TO THE PRESSING DIRECTION

Optical measurements were conducted on two commercial specimens of Lucalox (G.E. Co.). One specimen was forged (1850°C, 15 kpsi in 180 minutes, and 5.4% reduction - FA-132) and the other was measured in the "as-received" condition (both samples were given an equivalent optical polish). The total and in-line transmission as a function of wavelength is plotted in Figure 27, and the transparency of the specimens are illustrated pictorially in Figure 28. It was expected that the forging might induce crystallographic texture in the sample and increase in-line transmission, but this expectation was not fulfilled. Instead, the in-line transmission was equal for the two specimens. However, the forged specimen possessed a somewhat increased total transmission (the difference in thickness accounts for only 1.5% of the increased transmission). This suggests that the hot forging process itself is capable of porosity removal on this material (see Section II.C for discussion of several possible mechanisms under this general category).

E. Critical Strain Experiments

The discussion in Section I mentioned the fact that a critical strain exists for maximum crystal growth. With suitable control of the nucleation step, it should be possible to grow large single crystals, and in fact this is commonly done with metals.[2] The determination of the critical strain for maximum crystal growth was attempted, and although the question has not been definitively answered, significant progress has been made. It was thought from previous work[1] that the critical strain was between 2 and 10 percent. The program plan was to produce a number of specimens uniformly strained within this range, and then to subject each specimen to a uniform nucleation-and-growth thermal treatment. From an examination of the grain size of these specimens, it was thought that the "critical strain" could be determined. This phase of

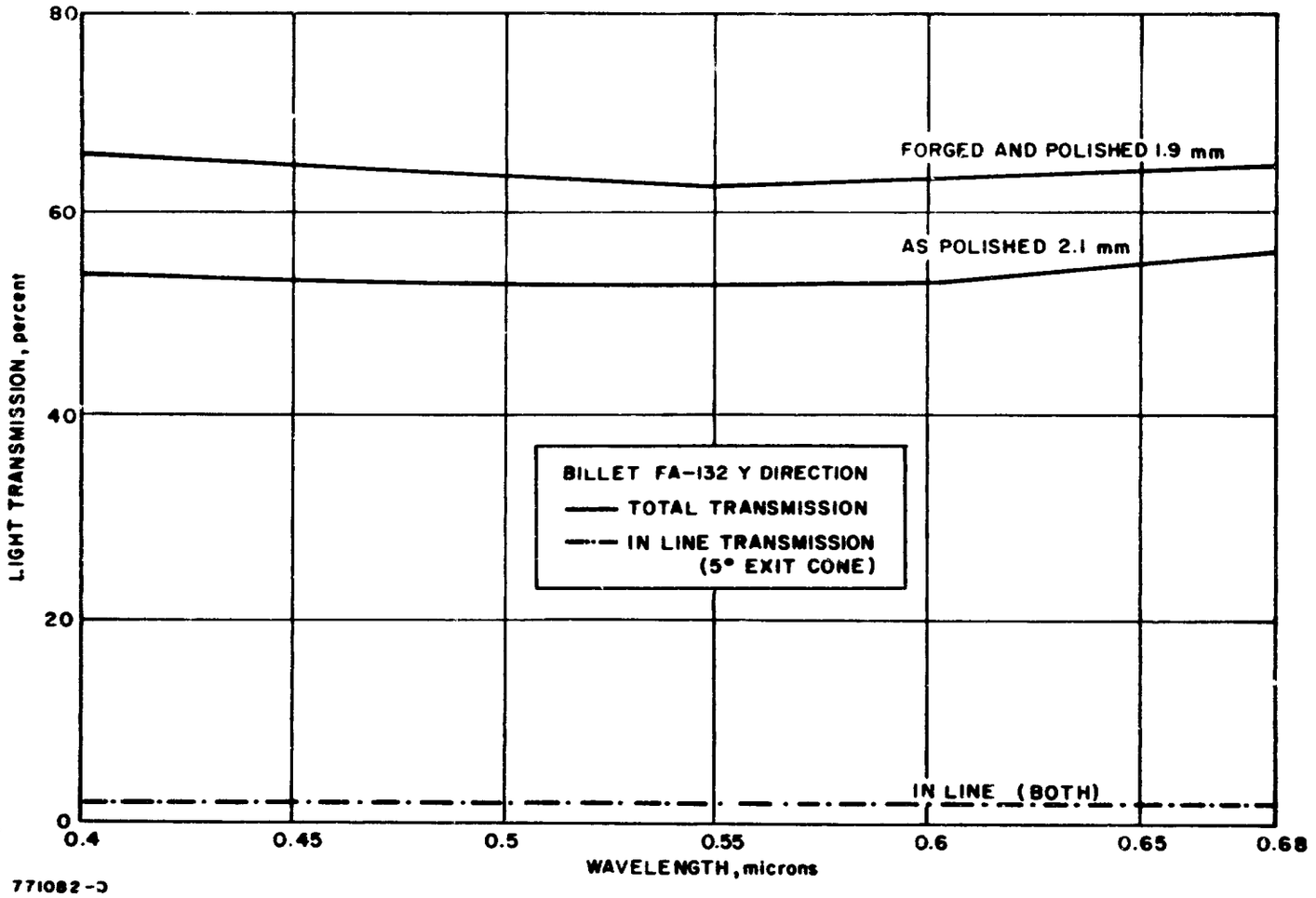

Figure 27 TOTAL AND IN-LINE TRANSMISSION FOR AS-RECEIVED AND FORGED LUCALOX

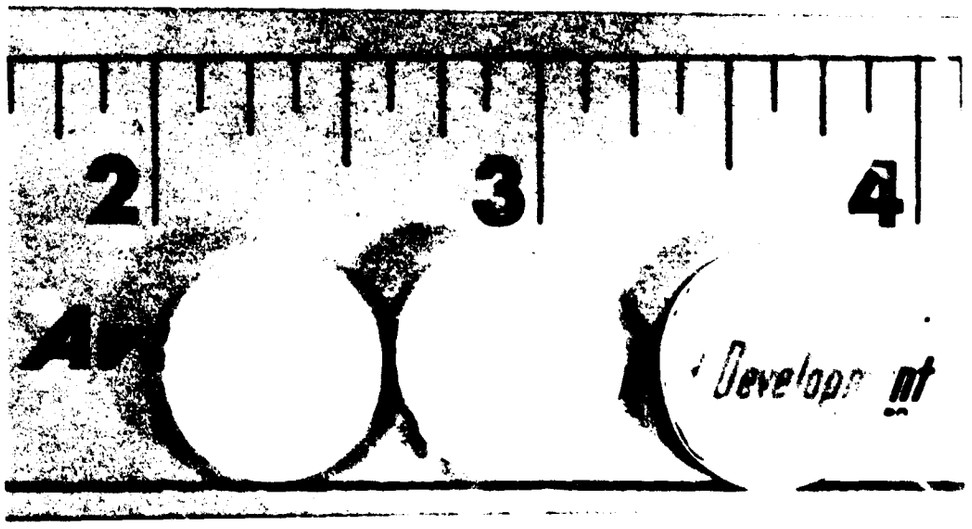

Figure 28. Lucalox (G.E.) alumina illustrating transparency for specimens from left to right; as fired, as polished, FA-132 forged and polished.

the program was only partially completed, so the following remarks should be viewed as a progress report.

The apparatus used for forging is shown in Figure 29. This consisted essentially of a water cooled fused quartz envelope and a pressure train made up as follows: tungsten/alumina piston/5 mil molybdenum sheet/alumina specimen. It was "O" ring sealed so that an argon atmosphere could be maintained. A 7/16 inch diameter specimen was used for this work.

With a 5 KW induction generator coupled to the molybdenum sheet on either side of the specimen, temperatures up to the melting point of alumina (2050°C) were achieved. It was hoped that with this short ($7\frac{1}{2}$ inch) pressure train and the clear view of the specimen, deformation control could be achieved by means of a cathetometer and/or dial gage mounted to the press platens; the deformation monitoring attempts were only moderately successful.

The forgings and results are listed in Table 3. The starting material for the forgings was pure (99.98%) alumina which had been conventionally hot pressed to greater than 99.5% of theoretical density. A number of strains in the desired range were achieved, and in many cases the deformations were uniform. Most of these forgings were conducted above 1700°C which is undoubtedly above the recrystallization temperature of alumina, so it was thought necessary to quench these specimens to some relatively low temperature - 1000° to 1200°C - to prevent recrystallization; recrystallization was to be induced subsequently in a controlled manner. Quenching was accomplished while pressure was being maintained which should have inhibited the formation of any strain-free nuclei.

Many forgings were conducted at 1760°C and deformations up to 10 percent were achieved. No firm conclusion can be drawn relating pressure and deformation, as each run was terminated to achieve a specified deformation--thus times at load varied considerably. In the forging process, the aspect ratio of the

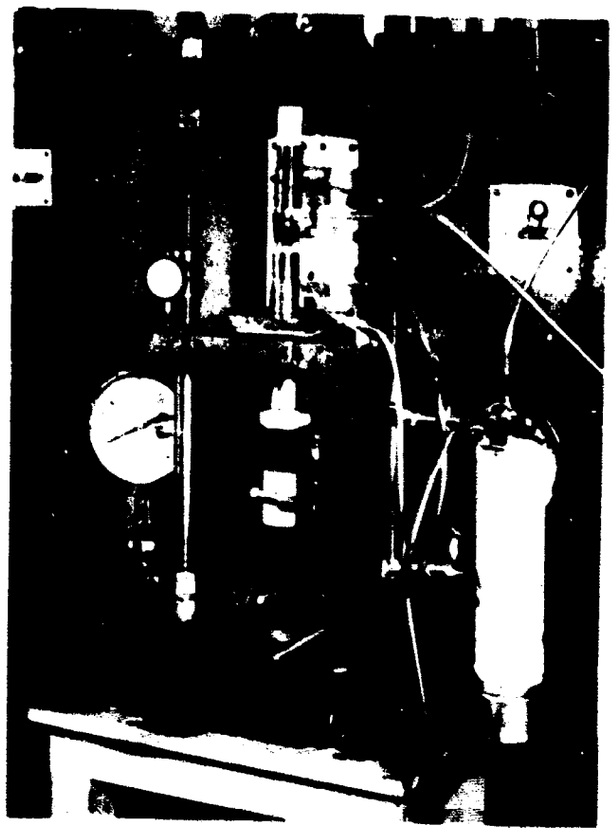

Figure 29. Forging Apparatus for Critical Strain Experiments.

Table 3.

Forgings of Small Specimens for Annealing Experiments

Specimen No.	Temp. °C	Pressure kpsi	Percent Height Reduction	Post Strain Treatment
JC 2	1760	5.8	2	Quench and reheat to 1810°C
JC 3	1760		4.5	Quench to 23°C
JC 6	1760	8.7	10	Quench to 1000°C, furnace cool
JC 12	1770	3.0	0	Quench to 1200°C, furnace cool
JC 13	1500	run terminated prematurely		
JC 14	1770	5.0	0.2	Quench to 1200°C, furnace cool
JC 15	1500	run terminated prematurely		
JC 16	1800	7.5	1.5	Quench to 1200°C, furnace cool
JC 17	1760	13.5	1.8	Quench to 1200°C, furnace cool
JC 19	1770	0.7	0	Quench to 1260°C, furnace cool
JC 20	1760	5.0	1.4	Quench to 1215°C, furnace cool
JC 21	1760	8.0	1.4	Quench to 1200°C, furnace cool
JC 22	1850	8.0	20	Furnace cooled
JC 23	1860	8.0	4	Quench to 1235°C, furnace cool
JC 24	1800	6.0	3.8	Quench to 1200°C, furnace cool

specimen is the most important variable to control after temperature and pressure.[7] A convincing demonstration of this was obtained by comparing the results for forging JC-22 (aspect ratio of 0.45) and JC-23 (aspect ratio of 0.09). Both forgings were conducted at the same pressure and temperature, yet JC-22 deformed greater than 20 percent in less than 1 minute and JC-23 took 20 minutes to deform 4 percent. The amount of shearing forces as compared to hydrostatic force increases with the aspect ratio and this promotes plastic deformation by slip.

The program plan called for these samples to be given a uniform recrystallization treatment. It was decided to pass the specimens through a temperature gradient which included the recrystallization temperature at a specified rate and then hold them in a uniform temperature zone for 1 hour. This cycle is shown in Figure 30.

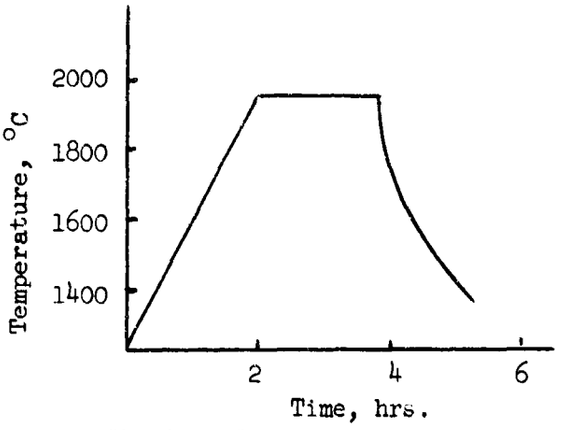

Figure 30. Standard Thermal Cycle for Strain-Anneal Experiments

Much of the time spent on this aspect of the program was concerned with the design and debugging of an apparatus to produce the desirec thermal treatment. The final design is shown schematically in Figure 31. A Lepel Crystal Puller provided a means of uniform lowering and consequently a means for heating a specimen at a constant rate. Slots were cut in the susceptor to introduce

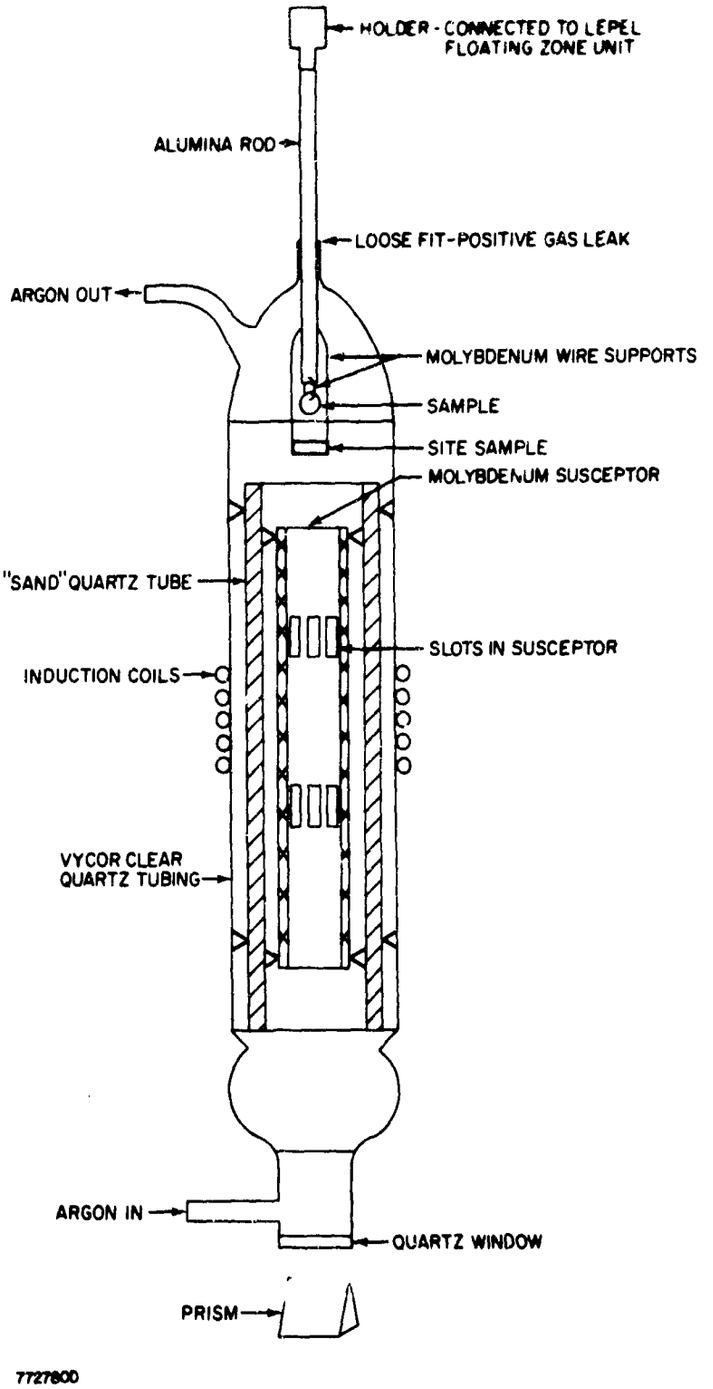

Figure 31 TEMPERATURE GRADIENT ANNEALING FURNACE

a sharp temperature gradient. The temperature at the hot zone was held at the final annealing temperature throughout the anneal. A site sample (alumina) was lowered ahead of the forged specimen so final temperature adjustments could be made. An argon protective atmosphere was maintained within the chamber. No completely successful annealing has as yet been completed although several moderately successful annealings have been completed. Specimen JC-24 was annealed according to the above mentioned heating cycle although it did not undergo the full 2 hours at 1950°C. A microstructural examination of the anneal specimen failed to reveal any evidence of single crystal growth or recrystallization. The preliminary conclusion is that 3.8% strain is below the critical strain.

One series of forgings (JC-4 and JC-7-11) was conducted at a temperature which was believed to be below the recrystallization temperature of Al_2O_3 and these are reported in Table 4. Forging at low temperatures is attractive in that the quench step and the uncertainty of preventing recrystallization would be eliminated. The working and recrystallization steps would in this case be analogous to those used in conventional metallurgical practice. The experiments were intended to show the limits of temperature and pressure which could be employed for the hot working of Al_2O_3. It was recognized that die material limitations rendered pressures in the range of 35 kpsi impractical for large (1 inch diameter) specimens. These forgings were $\frac{1}{5}$ inch diameter specimens using SiC punches and a platinum furnace. All of the specimens exhibited some reaction with the SiC punches and consequently cracked into several pieces. However, it is thought to be quite significant that homogeneous deformation was achieved which implies that five independent plastic flow systems (Von Mises criteria[11]) were operative. Although little crystallographic texturing was

Table 4.

Low Temperature Forgings of Small Specimens

Specimen No.	Temp. °C	Pressure kpsi	Percent Height Reduction	Post Strain Treatment
JC 4	1350	35.0	4	Furnace cool
JC 7	1350	35.0	1.5	Furnace cool
JC 8	1350-1500	35.0	45	Furnace cool
JC 9	1425	35.0	50	Furnace cool
JC 10	1425	35.0	35	Furnace cool
JC 11	1425	35.0	37	Furnace cool

observed, some microstructural texturing occurred (Figures 32 a and b). There was no evidence that recrystallization had proceeded--thus it appears that these specimens were in fact forged below the recrystallization temperature. Thus, it appears that critical strain annealing experiments could be done with these specimens.

F. Mechanical Properties

A limited study was made of the brittle strengths of some of the more transparent specimens. This data is listed in Table 5 and also plotted in Figure 33. The strength of polycrystalline alumina depends critically on grain size. Data from Spriggs, Mitchell, and Vasilos[12] are included in this figure for comparison. It can be seen that the strengths of the transparent, [illegible] μ grain size alumina is intermediate between the 40-50 μ and 80-100 μ grain size opaque materials. Also, the room temperature values agree closely with those of Charles and Shaw[13] for Lucalox (G.E. translucent polycrystalline Al_2O_3). This suggests that neither the press forging nor the transparency has seriously weakened the specimens produced under the present program. Moreover,

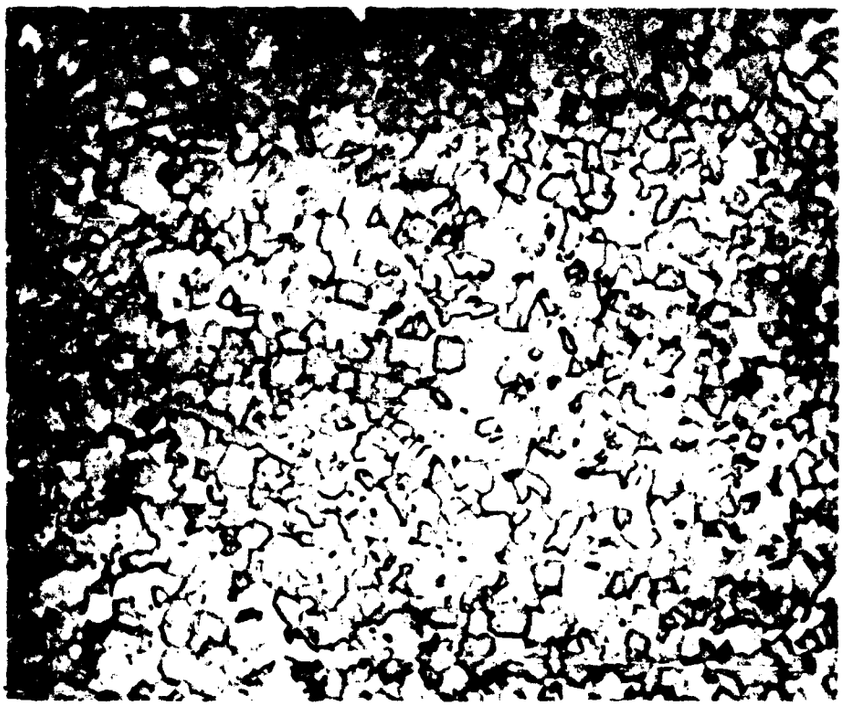

4216 B (a) 1000 X

4216 A (b) 1000 X

Figure 32. Microstructural texture in relatively low temperature press forged alumina (a) parallel, and (b) perpendicular to press forging direction.

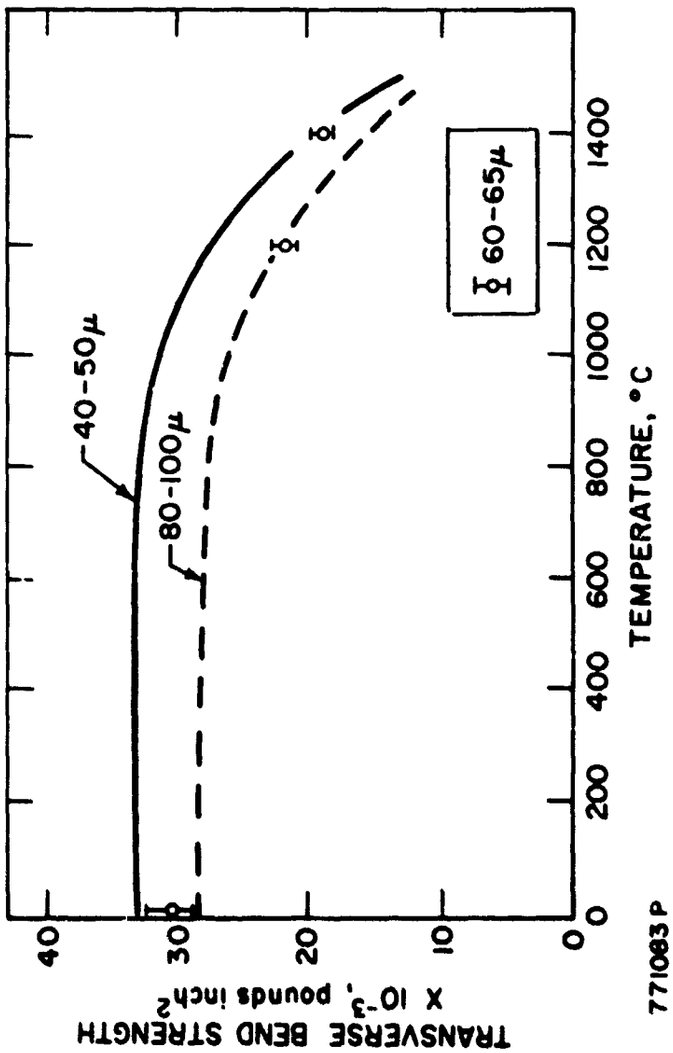

Figure 33 TRANSVERSE BEND STRENGTH OF TRANSPARENT ALUMINA VERSUS TEMPERATURE. SOLID CURVES REPRESENT DATA FOR DENSE BUT OPAQUE ALUMINA[13]

Table 5.

Bend Strengths of Transparent Polycrystalline Alumina
(Billet FA 10_)

Temperature	Bend Strength (psi)
23°C	29.2
	32.2
	31.9
	28.6
1200°C	21.5
	21.9
	21.6
	21.5
1400°C	19.5
	18.4
	18.8

it may be expected that experience with and trends predicted from opaque alumina may be extended to transparent alumina, at least with regard to their mechanical properties. Such experience would suggest that finer ultimate grain sizes would be desirable for improved strengths and this is expected to depend critically on the post recrystallization heat treatment.

III. SUMMARY

A. Three types of high purity Al_2O_3 powders varying from 0.06 μ to 0.3 μ average particle size were used successfully to produce highly transparent bodies by a hot forging and annealing technique. Sintering or pressure sintering performed on the powder before the application of the forging pressure was found to be detrimental because it led to a retention of porosity in the finished product. Suitable annealing periods were established at 2 to 6 hours. The amount of transparent area in a billet was found to be influenced by the presence of strain gradients, which in turn were found to be related to the aspect ratio, surface friction, creep behavior of mating materials, and the strain rate

employed. Solid billet forgings necessitated the use of higher pressure levels to achieve a given deformation, because of larger initial grain sizes, and, in general, were found to offer no advantages over the powder forging technique.

B. The hot working of alumina results in a strong basal crystallographic texture normal to the pressing direction, principally because of the dominance of a basal slip deformation mechanism. This same texture is retained after recrystallization, and this may be due to an oriented nucleation mechanism of recrystallization. The recrystallized material exhibits microstructural texture after an extensive growth period, and this was attributed to oriented grain growth.

C. A pore removal mechanism thought to be unique to the hot working process accompanies deformation and/or primary recrystallization. Several deformation pore removal mechanisms, such as the shearing of pores due to grain boundary sliding and recrystallization pore removal mechanisms, such as the nucleation of the new population of grains at pores, are thought to be responsible for the development of transparency.

D. The in-line transmission of forged alumina at optical frequencies was found to be considerably higher (with values up to 60%) than randomly oriented pore-free polycrystalline alumina. This improvement is thought to be a result of crystallographic texturing. Total transmission values of material generated during this study were equivalent to the best randomly oriented polycrystalline alumina.

E. A series of specimens were forged and quenched for use in annealing experiments which were designed to study the critical strain required for primary recrystallization. Initial experiments indicated that the critical strain was above 3.8%. Microstructural texture was produced in small scale forgings conducted at considerably lower temperatures (1400°C) than normally

employed (1850°C) by going to very high pressures (35 kpsi).

F. Bend strengths of transparent specimens at 23°C, 1200°C, and 1400°C were found equivalent to dense but opaque specimens of equivalent grain size.

IV. CONCLUSIONS AND RECOMMENDATIONS

Polycrystalline Al_2O_3 possessing total light transmission of greater than 75% and in-line light transmission of greater than 55% in the visible range can be prepared by the hot forming techniques described in this report. Unique pore removal mechanisms active during the deformation and recrystallization periods are thought to be responsible for the transparency achieved. The high in-line transmission hereto not possible in this anisotropic material is a result of the strong crystallographic texture induced by the basal slip of this material at very high temperatures.

Presently, the process is limited in reliability and to the realization of small (< 4 square inch) area tiles. The consistent extension of these techniques to larger areas requires a better understanding of the following categories.

1. Determination of Optimum Raw Material Characteristics - The techniques employed provided transparent material with all three powders that were examined; i.e., the process seems to hold a certain latitude in the choice of starting material. However, it is felt that to further improve total transmission values to levels beyond 80% transmission, the influence of variations in powder characteristics such as particle size and impurity levels on transparency will have to be established.

2. Modifications of the hot forming technique will have to be developed to consistently produce a uniform deformation over a greater percentage of the billet area. The proper control of this parameter would extend the size of transparent areas within each billet.

3. A better understanding of the pore removal mechanism(s) active during the deformation and annealing periods and factors which directly influence their effectiveness would be useful to establish more optimum processing conditions.

4. Greater plastic deformation and therefore greater preferred crystallographic orientation must be achieved to increase the thickness of material through which distant objects may be viewed clearly.

APPENDIX

Since there is a lack of standardization of qualifying terms used in the study of optics, the following definitions of optical terms are included and are appropriate to the terms discussed within this text.

Opaque - inpenetrable to light, not allowing light to pass through.

Translucent - having the property of transmitting rays of light to pass through but diffusing it so that persons, objects, etc. on the opposite side are not clearly visible.

Transparent - having the property of transmitting rays of light through its substance so that bodies situated beyond or behind can be distinctly seen.

Total Transmission - transmittance, the ratio of the radiant flux transmitted through and emerging from a body to the total flux incident to it.

In-Line Transmission - transmittance of emergent beam which is parallel to the entrance beam, sometimes called specular transmittance. In the reported text, a 5° exit cone whose axis is parallel to the entrance beam was evaluated to arrive at the stated values.

Diffuse Transmission - light transmission passing through a body irrespectful of the 5° parallel exit cone - total transmission minus the in-line transmission.

REFERENCES

1. W.H. Rhodes, D.J. Sellers, T. Vasilos, A.H. Heuer, R. Duff, and P. Burnett "Microstructure Studies of Polycrystalline Refractory Oxides," D.J. Sellers, W.H. Rhodes, and T. Vasilos, "Single Crystal Alumina Grown by Strain Anneal," Summary Reports, Contract NOw-65-0316-f (March 24, 1966).

2. K.T. Aust, The Art and Science of Growing Crystals, edited by J.J. Gilman, p. 452, Wiley & Sons, New York (1963).

3. R.B. Day and R.J. Stokes, J. Am. Ceram. Soc., 47 (10), p. 493 (1964).

4. R.W. Rice and J.G. Hunt, "Hot Extrusion of MgO" presented at 66th Annual Meeting, Am. Ceram. Soc., Chicago, Illinois (April 1964).

5. R.W. Cahn, "Recovery and Recrystallization" in Physical Metallurgy, edited by R.W. Cahn, North Holland Publishing Co. (1965).

6. R.W. Cahn, "Recrystallization Mechanisms," in Recrystallization, Grain Growth and Textures, Am. Society for Metals (1966).

7. A.H. Heuer, W.H. Rhodes, D.J. Sellers, and T. Vasilos, "Microstructure Studies of Polycrystalline Refractory Oxides," Contract NOw-66-0506-(d), AVSSD-0211-67-RR, Summary Report (April 1967).

8. "Optical Properties of Synthetic Sapphire," Technical Release of Union Carbide Corporation, Linde Division.

9. R.L. Coble, J. Am. Ceram. Soc., 41 55(1958).

10. T. Vasilos and R.M. Spriggs, Prog. Ceram. Sci., 4, 95 (1966).

11. G. Groves and A. Kelley, Phil. Mag., 8, 877 (1963).

12. R.M. Spriggs, J.B. Mitchell, and T. Vasilos, J. Am. Ceram. Soc., 47, (4), 203-4 (1964).

13. R.J. Charles and R.R. Shaw, "Delayed Failure of Polycrystalline and Single-Crystal Alumina," G.E. Research Report 62-RL-3081M.

UNCLASSIFIED

Security Classification

DOCUMENT CONTROL DATA - R&D

(Security classification of title, body of abstract and indexing annotation must be entered when the overall report is classified)

1 ORIGINATING ACTIVITY *(Corporate author)*

Avco Corporation, Space Systems Division,
Lowell Industrial Park, Lowell, Massachusetts

2a. REPORT SECURITY CLASSIFICATION

Unclassified

2b GROUP

3 REPORT TITLE

Development and Evaluation of Transparent Aluminum Oxide

4 DESCRIPTIVE NOTES *(Type of report and inclusive dates)*

Final Report - 1 July 1966 - 30 June 1967

5 AUTHOR(S) *(Last name, first name, initial)*

Rhodes, William H. Heuer, Arthur H.
Sellers, David J. Vasilos, Thomas

6 REPORT DATE	7a. TOTAL NO. OF PAGES	7b. NO. OF REFS
June 30, 1967	68	13

8a. CONTRACT OR GRANT NO.	9a. ORIGINATOR'S REPORT NUMBER(S)
N178-8986	Final Technical Report
b. PROJECT NO.	
c.	9b. OTHER REPORT NO(S) *(Any other numbers that may be assigned this report)*
d	

10 AVAILABILITY/LIMITATION NOTICES

Distribution of this document is unlimited.

11. SUPPLEMENTARY NOTES	12. SPONSORING MILITARY ACTIVITY
	U.S. Naval Weapons Laboratory Dahlgren, Virginia 22448

13 ABSTRACT

Polycrystalline Al_2O_3 possessing high total and in-line transmission in the visible range was prepared successfully by a combined high temperature hot forging and annealing operation. Transparency was found to be produced by a combination of several pore removal mechanisms active during deformation and primary recrystallization. A strong basal texture normal to the pressing direction was found for both deformation and recrystallization structures, and the high in-line transmission characteristics were thought to be due to a lowering of birefringent scattering because of this texture. Initial experiments were conducted to define the critical strain for recrystallization, and to date it is thought that this strain lies between 4 and 10 percent. Room and elevated temperature bend strengths of these materials were equivalent to opaque but dense pressure or pressureless sintered alumina having a comparable grain size.

DD FORM 1 JAN 64 1473

UNCLASSIFIED

Security Classification

14. KEY WORDS	LINK A		LINK B		LINK C	
	ROLE	WT	ROLE	WT	ROLE	WT
Alumina						
Transparency						
Hot Working						
Press Forging						
Pore Removal						
Texture						
Primary Recrystallization						
Mechanical Properties						

INSTRUCTIONS

1. **ORIGINATING ACTIVITY:** Enter the name and address of the contractor, subcontractor, grantee, Department of Defense activity or other organization *(corporate author)* issuing the report.

2*a*. **REPORT SECURITY CLASSIFICATION:** Enter the overall security classification of the report. Indicate whether "Restricted Data" is included. Marking is to be in accordance with appropriate security regulations.

2*b*. **GROUP:** Automatic downgrading is specified in DoD Directive 5200.10 and Armed Forces Industrial Manual. Enter the group number. Also, when applicable, show that optional markings have been used for Group 3 and Group 4 as authorized.

3. **REPORT TITLE:** Enter the complete report title in all capital letters. Titles in all cases should be unclassified. If a meaningful title cannot be selected without classification, show title classification in all capitals in parenthesis immediately following the title.

4. **DESCRIPTIVE NOTES:** If appropriate, enter the type of report, e.g., interim, progress, summary, annual, or final. Give the inclusive dates when a specific reporting period is covered.

5. **AUTHOR(S):** Enter the name(s) of author(s) as shown on or in the report. Enter last name, first name, middle initial. If military, show rank and branch of service. The name of the principal author is an absolute minimum requirement.

6. **REPORT DATE:** Enter the date of the report as day, month, year; or month, year. If more than one date appears on the report, use date of publication.

7*a*. **TOTAL NUMBER OF PAGES:** The total page count should follow normal pagination procedures, i.e., enter the number of pages containing information.

7*b*. **NUMBER OF REFERENCES:** Enter the total number of references cited in the report.

8*a*. **CONTRACT OR GRANT NUMBER:** If appropriate, enter the applicable number of the contract or grant under which the report was written.

8*b*, 8*c*, & 8*d*. **PROJECT NUMBER:** Enter the appropriate military department identification, such as project number, subproject number, system numbers, task number, etc.

9*a*. **ORIGINATOR'S REPORT NUMBER(S):** Enter the official report number by which the document will be identified and controlled by the originating activity. This number must be unique to this report.

9*b*. **OTHER REPORT NUMBER(S):** If the report has been assigned any other report numbers *(either by the originator or by the sponsor)*, also enter this number(s).

10. **AVAILABILITY/LIMITATION NOTICES:** Enter any limitations on further dissemination of the report, other than those imposed by security classification, using standard statements such as:

(1) "Qualified requesters may obtain copies of this report from DDC."

(2) "Foreign announcement and dissemination of this report by DDC is not authorized."

(3) "U. S. Government agencies may obtain copies of this report directly from DDC. Other qualified DDC users shall request through _____ _____."

(4) "U. S. military agencies may obtain copies of this report directly from DDC. Other qualified users shall request through _____."

(5) "All distribution of this report is controlled. Qualified DDC users shall request through _____."

If the report has been furnished to the Office of Technical Services, Department of Commerce, for sale to the public, indicate this fact and enter the price, if known.

11. **SUPPLEMENTARY NOTES:** Use for additional explanatory notes.

12. **SPONSORING MILITARY ACTIVITY:** Enter the name of the departmental project office or laboratory sponsoring *(paying for)* the research and development. Include address.

13. **ABSTRACT:** Enter an abstract giving a brief and factual summary of the document indicative of the report, even though it may also appear elsewhere in the body of the technical report. If additional space is required, a continuation sheet shall be attached.

It is highly desirable that the abstract of classified reports be unclassified. Each paragraph of the abstract shall end with an indication of the military security classification of the information in the paragraph, represented as *(TS)*, *(S)*, *(C)*, or *(U)*.

There is no limitation on the length of the abstract. However, the suggested length is from 150 to 225 words.

14. **KEY WORDS:** Key words are technically meaningful terms or short phrases that characterize a report and may be used as index entries for cataloging the report. Key words must be selected so that no security classification is required. Identifiers, such as equipment model designation, trade name, military project code name, geographic location, may be used as key words but will be followed by an indication of technical context. The assignment of links, rules, and weights is optional.